Acta Crystallographica Section B
Structural Science
ISSN 0108-7681

Crystal chemistry of zirconosilicates and their analogs: topological classification of MT frameworks and suprapolyhedral invariants

G. D. Ilyushin[a]* and V. A. Blatov[b]

[a]Institute of Crystallography of RAS, Leninsky Pr. 59, Moscow 117333, Russia, and [b]Samara State University, Ac. Pavlov St. 1, Samara 443011, Russia

Correspondence e-mail: ilyushin@mail.ru

Received 22 August 2001
Accepted 17 December 2001

The first attempt is undertaken to consider systematically topological structures of zirconosilicates and their analogs (60 minerals and 34 synthetic phases), where the simplest structure units are MO_6 octahedra and TO_4 tetrahedra united by vertices ($[TO_4]$:$[MO_6]$ = 1:1–6:1). A method of analysis and classification of mixed three-dimensional *MT* frameworks by topological types with coordination sequences $\{N_k\}$ is developed, which is based on the representation of crystal structure as a finite 'reduced' graph. The method is optimized for the frameworks of any composition and complexity and implemented within the *TOPOS*3.2 program package. A procedure of hierarchical analysis of *MT*-framework structure organization is proposed, which is based on the concept of polyhedral microensemble (PME) being a geometrical interpretation of coordination sequences of *M* and *T* nodes. All 12 theoretically possible PMEs of MT_6 polyhedral composition are considered where *T* is a separate and/or connected tetrahedron. Using this methodology the *MT* frameworks in crystal structures of zirconosilicates and their analogs were analyzed within the first 12 coordination spheres of *M* and *T* nodes and related to 41 topological types. The structural correlations were revealed between rosenbuschite, lavenite, hiortdahlite, woehlerite, siedozerite and the minerals of the eudialyte family.

1. Introduction

Silicates traditionally form one of the most popular classes of inorganic compounds considered valuable in validating new models of crystal structures or new methods of crystallochemical analysis (Bragg, 1930; Liebau, 1956, 1985; Belov, 1959, 1976; Zoltai, 1960; Kostov, 1971; Puschcharovskii, 1986; Bokij, 1998). In turn, the most developed part in theoretical crystal chemistry of silicates is the class of framework aluminosilicates, which can be divided into two subclasses; homogeneous with only *T* tetrahedra as the ***primary building units***[1] (PBU), and heterogeneous (or mixed) frameworks with *T* tetrahedra and *M* octahedra as PBUs. Special attention in the crystal chemistry of silicates is paid to the first largest family of tetrahedral zeolite-like structures, which were classified mainly in two different ways.

In a number of works (Meier, 1968; Breck, 1974; Meier & Moeck, 1979; Barrer, 1982; Liebau, 1985; Smith, 1988; Bokij, 1998) the concept of the *secondary building unit* (SBU) as a stable and typical union of PBUs was used in classification. Meier (1968) proposed an initial set of six SBUs containing from four up to 12 tetrahedra, which can be found in all the

[1] Hereinafter the definitions of the concepts marked as bold italic are given in the *Appendix*.

frameworks of the zeolite structural types known at that time. Breck (1974) enlarged that list up to seven SBUs. Meier & Moeck (1979) separated nine different SBU types for all known synthetic and natural tetrahedral structures of zeolite-like aluminosilicates. Smith (1988) adduced complete data on topological parameters of 30 natural and 16 synthetic zeolites and indicated all possible types of ring fragments for each of them. He also considered the variants of condensing SBUs to infinite one-dimensional chains or two-dimensional layers, however, having specified such groups for some zeolites. Bokij (1998) described 16 SBUs in natural zeolites and conditionally divided them into six main and ten additional units, which were not used in the classification. However, at present there is no strict algorithm of separating SBUs or other building units, and no common criterion of referring to structural units as main or additional. Often SBUs cannot be separated in phases with complicated framework topology. In particular, SBUs had not been classified until now for feldspar-like T frameworks $A_x(TO_2)_y$ (A = Li, Na, K, Rb, Cs; T = Si, Al) and $B_x(TO_2)_y$ (B = Ca, Sr, Ba; Liebau, 1985; Smith, 1988; Bokij, 1998).

The second method was initiated by Meier & Moeck (1979), who proposed the classification of zeolites on the basis of sets of n numbers $\{N_k\}$, k = 1–n, so-called ***coordination sequences*** (CS; Brunner & Laves, 1971) for a ***connected substructure*** of T atoms calculated to a given depth of n coordination spheres (n = 5 was accepted). Besides, Meier & Moeck (1979) applied CSs for crystallographically different T atoms (T nodes) in a given framework to determine their topological equivalence: the equality of CSs for T atoms indicated the presence of additional 'topological' framework symmetry. Having arranged the crystal structures of 31 synthetic and natural zeolites in ascending order of $\{N_k\}$ (k = 1–5), Meier & Moeck (1979) revealed that N_k values were identical for four pairs of zeolites (RHO/LTA,[2] KFI/GME, ERI/OFF and MER/PHI) characterized by different SBU types and, hence, by different framework topologies. Thus, it was shown that the equality of CSs for corresponding T atoms in T frameworks to be compared is a necessary but not sufficient condition of their topological identity. This paper stimulated a new trend of investigations of CS properties for T atoms in zeolite frameworks (Stixrude & Bukowinski, 1990; O'Keeffe, 1995; Grosse-Kunstleve *et al.*, 1996). At present CSs are accepted as one of the most important topological characteristics of zeolites and are calculated up to n = 10 (Meier *et al.*, 1996). The following CS features stipulate the advantages of this classification method:

(i) unambiguity and relative non-complexity of the calculation;

(ii) simplicity of comparing CSs of crystal structures to be classified;

(iii) possibility of combining a local and global approach to crystal structure description: although, strictly speaking, CS is determined on a finite crystal structure fragment, the equality of two $\{N_k\}$, k = 1–n, indicates that structure isomorphism is already at n = 3–5, as a rule (Meier & Moeck, 1979; Blatov, 2000).

At the same time the two approaches mentioned above (further abbreviated to SBU and CS methods for short) were mainly used to classify homogeneous silicates with T-PBUs or T substructure. An unsolved problem, which a number of authors (Zoltai, 1960; Kostov, 1971; Liebau, 1985) noticed, is a consideration of other important silicate components, first of the most typical M atoms with octahedral coordination in ***MT frameworks*** and second the corresponding development of existing classification schemes.

2. A brief chemical and topological characterization of *MT* frameworks

The silicate group of MT frameworks represents a less theoretically investigated family to be formed by vertex condensation of M octahedra $[MO_6]$ and T tetrahedra $[TO_4]$. The voids in MT frameworks are randomly (Hong, 1976; Ilyushin *et al.*, 1981*c*,*d*) or orderly (Ilyushin *et al.*, 1981*a*,*b*) occupied by alkali (A) or alkaline-earth (B) cations. The possibility of wide isomorphous substitutions in the $A(B)$ sublattice (including the substitution $2A \leftrightarrow 1B$ as in feldspars) determines their similarity to zeolites and use as molecular sieves, effective ion-exchangers and solid electrolytes (Hong, 1976; Ilyushin & Demianets, 1989, 1996; Poojary *et al.*, 1997; Jale *et al.*, 1999; Lin *et al.*, 1999; Cheetham *et al.*, 1999; Rocha & Anderson, 2000; Ferreira *et al.*, 2001; Clearfield, 2001).

Several attempts have already been undertaken to select SBUs composing of M and T polyhedra in crystal structures of various compounds, not only silicates (Hawthorne, 1983, 1985, 1990, 1994; Ilyushin, 1989; Ilyushin & Demianetz, 1989, 2001), whereas the CS method was never used for them. Note that the topological description of MT framework structural features becomes complex in comparison with tetrahedral frameworks because of the appearance of two types of six- and four-connected nodes in three-dimensional nets and the polyvariant condensation of M octahedra with each other and with T tetrahedra. This condensation can be realised both by vertices which are typical for zeolites and by edges (M–M or M–T types).

In this study we have undertaken the first attempt of systematic consideration of characteristic structural features of zirconosilicates and their analogs $A(B)_xMT_yO_z{\cdot}mH_2O{\cdot}hX$ (50 minerals and 34 synthetic phases), with A = Li–Cs; B = Ca–Ba; M = Zr, Sn, Ti, Si; T = Si, Ge; X = Cl, F, OH; x = 1–8, y = 1–6, m = 0–3, h = 1–2, using the CS method. Zirconosilicates form their own crystallochemically interesting and numerous family of MT frameworks owing to the great crystal structure complexity determined by the system rank that R are equal to the number of chemical types of atoms, and by the various ways of their binding. The rank of chemical systems to which framework zirconosilicates belong is rather high: it varies from 4 (3 for some silicon analogs) up to 5–6 and for some minerals, even without consideration of positional isomorphism, it

[2] Hereinafter we use, for the designation of a framework, three-letter abbreviations which are accepted in the crystal chemistry of zeolites (Meier *et al.*, 1996).

Table 1
List of all studied zirconosilicates and their analogs grouped by the complexity rank of their chemical composition and by topological families.

Column headed No. represents the number of topological types or topological family.

No.	Compound	*w*	*q*	Mineral/synthetic	Structure type	Space group	Reference or collection code
R = 3–6							
1	$ZrSiO_4$	0	1.0	Zircon	ZIR	$I4_1/amd$	100248
2(*a*)	$LiNaZrSi_6O_{15}$	2.0	6.0	Zektzerite	ZEK	*Cmca*	100631
2(*b*)	$Li_2ZrSi_6O_{15}$	2.0	6.0	Synthetic	ZEK	*Cmca*	Quintana & West (1981)
3(*a*)	$Li_3KZr_2\ Si_{12}O_{30}$	2.0	6.0	Sogdianite	SOG	*P*6/*mcc*	10155
3(*b*)	$Li_3KSn_2Si_{12}O_{30}$	2.0	6.0	Brannockite	BRA	*P*6/*mcc*	202622
4	Na_2ZrSiO_5	2.0	1.0	Synthetic	ZrSi-1	$P2_1/c$	24866
5(*a*)	$Na_3Zr_2Si_2PO_{12}$	1.5	1.5	NASICON–L	NAS-L	*C*2/*c*	202154
5(*b*)	$Na_3Zr_2Si_2PO_{12}$	1.5	1.5	NASICON–H	NAS-H	$R\bar{3}c$	63567
5(*c*)	$Na_4Zr_2Si_3O_{12}$	2.0	1.5	NASICON	NAS	$R\bar{3}c$	38056
6(*a*)	$NaHZrSi_2O_7$	1.0	2.0	Keldyshite	KEL	$P\bar{1}$	20186
6(*b*)	$Na_2SiSi_2O_7$	2.0	2.0	Synthetic	pKEL	*C*2/*c*	81134
6(*c*)	$Na_2ZrSi_2O_7$	2.0	2.0	Parakeldyshite	pKEL	$P\bar{1}$	24866
6(*d*)	$K_2ZrSi_2O_7$	2.0	2.0	Khibinskite	KHI	$P2_1/b$	20100
7(*a*)	$Na_3HZrGe_2O_8$	3.0	2.0	Synthetic	MRW†	*I*2/*m*	Nosirev *et al.* (1974)
7(*b*)	$Na_3HZrSi_2O_8$	3.0	2.0	Synthetic	MRW†	?	Ilyushin *et al.* (1983)
8	$Na_2BaTi_2Si_4O_{14}$	3.0	2.0	Batisite	BAT	*Ima*2	60411
9(*a*)	$Na_4Zr_2Si_5O_{16}(H_2O)$	2.0	2.5	Synthetic	ZrSi-2	?	Ilyushin *et al.* (1983)
9(*b*)	$Na_4Sn_2Si_5O_{16}(H_2O)$	2.0	2.5	Synthetic	SnSi-1	*B*2/*b*	20551
10(*a*)	$Na_4Sn_2Ge_5O_{16}(H_2O)$	2.0	2.5	Synthetic	SnGe-1	*P*2	20545
10(*b*)	$Na_4Zr_2Ge_5O_{16}(H_2O)$	2.0	2.5	Synthetic	ZrGe-1	*P*2/*b*	20640
11(*a*)	$Na_2ZrSi_3O_9(H_2O)_3$	2.0	3.0	Hilairite	HIL	*R*32	20257
11(*b*)	$Na_5YZrSi_3O_9(H_2O)_6$	2.0	3.0	Sazykinaite	SAZ	*R*32	Khomyakov (1995)
11*c*	$Na_5YTiSi_3O_9(H_2O)_6$	2.0	3.0	Mineral M67	HIL	?	Khomyakov (1995)
11(*d*)	$CaZrSi_3O_9(H_2O)_3$	1.0	3.0	Calciohilairite	HIL	*R*32	Bokij (1996)
11(*e*)	$BaZrSi_3O_9(H_2O)_{2.5}$	1.0	3.0	Komkovite	KOM	*R*32	39541
12(*a*)	$Na_2ZrSi_3O_9(H_2O)_2$	2.0	3.0	Catapleite-L	CAT-L	*B*2/*b*	20267
12(*b*)	$Na_2ZrSi_3O_9(H_2O)_2$	2.0	3.0	Catapleite –H	CAT-H	$P6_3/mmc$	40874
12(*c*)	$CaZrSi_3O_9(H_2O)_2$	1.0	3.0	Ca-Catapleite	CAT	*B*2/*b*	Bokij (1981)
12(*d*)	$K_2SiSi_3O_9$	2.0	3.0	Synthetic	WAD	$P\ 6_3$/m	31201
12(*e*)	$K_2SnSi_3O_9$	2.0	3.0	Synthetic	WAD	$P6_3/m$	19027
12(*f*)	$K_2TiSi_3O_9$	2.0	3.0	Synthetic	WAD	$P6_3/m$	19025
12(*g*)	$K_2ZrSi_3O_9$	2.0	3.0	Wadeite	WAD	$P6_3/m$	24446
12(*h*)	$Rb_2SnSi_3O_9$	2.0	3.0	Synthetic	WAD	$P6_3/m$	19028
12(*i*)	$Rb_2TiSi_3O_9$	2.0	3.0	Synthetic	WAD	$P6_3/m$	19026
13	$Na_2SiSi_3O_9$	2.0	3.0	Synthetic	SiSi-1	$P2_1/n$	82410
14(*a*)	$NaKZrSi_3O_9(H_2O)_2$	2.0	3.0	Georgechaoite	GEO	$P2_1nb$	201843
14(*b*)	$Na_2ZrSi_3O_9(H_2O)_2$	2.0	3.0	Gaidonnayite	GAI	$P2_1nb$	201846
15	$Na_4Zr_2(Si_6O_{18})(NaCl)(H_2O)_2$	2.0	3.0	Petarasite	PET	*C*2/*m*	20150
16	$Na_2ZrSi_4O_{11}$	2.0	4.0	Vlasovite	VLA	*C*2/*c*	16981
17	$Na_2TiSi_4O_{11}$	2.0	4.0	Narsarsukite	NAR	*I*4/*m*	16899
18	$Na_2TiSi_4O_{11}(H_2O)_2$	2.0	4.0	Penkvilskite	PEN	*Pnca*	75932
19(*a*)	$Na_2CaZr_2Si_{10}O_{26}(H_2O)$	3.0	5.0	Lemoynite	LEM	*C*2/*c*	41914
19(*b*)	$Na_3K_6Ti_2(Al_2Si_8O_{26})Cl_3$	4.5	5.0	Altisite	ALT	*C*2/*m*	79853
20	$Na_2ZrSi_6O_{15}(H_2O)_3$	2.0	6.0	Elpidite	ELP	*Pbcm*	10277
21	$Na_4H_4ZrSi_6O_{18}$	4.0	6.0	Terskite	TER	*Pnc*2	39454
22(*a*)	$Na_3H_5ZrSi_6O_{18}$	3.0	6.0	Lovozerite	LOV	*C*2	20595
22(*b*)	$Na_3H_3CaZrSi_6O_{18}$	4.0	6.0	Lovozerite	LOV	?	Khomyakov (1995)
22(*c*)	$Na_6CaZrSi_6O_{18}$	7.0	6.0	Zirsinalite	ZRS	$R\bar{3}c$	200800
22(*d*)	$Na_6CaTiSi_6O_{18}$	7.0	6.0	Koashvite	KOA	?	Khomyakov (1995)
22(*e*)	$Na_6MnTiSi_6O_{18}$	7.0	6.0	Kazakovite	KAZ	$R\bar{3}m$	200602
22(*f*)	$Na_6FeTiSi_6O_{18}$	7.0	6.0	Mineral M42	LOV	$R\bar{3}m$	Khomyakov (1995)
22(*g*)	$Na_8SiSi_6O_{18}$	8.0	6.0	Synthetic	LOV	$R\bar{3}$	85551
22(*h*)	$Na_8SnSi_6O_{18}$	8.0	6.0	Synthetic	LOV	$R\bar{3}m$	20804
22(*i*)	$Na_8SnSi_6O_{18}$	8.0	6.0	Synthetic	LOV	*C*2/*m*	20768
22(*j*)	$Na_8ZrSi_6O_{18}$	8.0	6.0	Synthetic	LOV	$R\bar{3}m$	Ilyushin *et al.* (1983)
22(*k*)	$Na_8ZrSi_6O_{18}$	8.0	6.0	Mineral M39	LOV	?	Khomyakov (1995)
23	$K_2ZrSi_3O_9(H_2O)$	2.0	3.0	Kostylevite	KOS	$P2_1/b$	20147
24(*a*)	$K_2ZrSi_3O_9(H_2O)$	2.0	3.0	Umbite	UMB	$P2_12_12_1$	83627
24(*b*)	$K_2TiSi_3O_9(H_2O)$	2.0	3.0	Synthetic	UMB	$P2_12_12_1$	83587
24(*c*)	$K_2SnSi_3O_9(H_2O)$	2.0	3.0	Synthetic	UMB	$P2_12_12_1$	Lin *et al.* (1999)
24(*d*)	$Na_2ZrSi_3O_9(H_2O)$‡	2.0	3.0	Synthetic	UMB	$P2_12_12_1$	84314
24(*e*)	$CsNaZrSi_3O_9(H_2O)$‡	2.0	3.0	Synthetic	UMB	$P2_12_12_1$	84315
24(*f*)	$CsKZrSi_3O_9(H_2O)$‡	2.0	3.0	Synthetic	UMB	$P2_12_12_1$	84312
25(*a*)	$K_2TiSi_6O_{15}$	2.0	6.0	Davanite	DAV	$P\bar{1}$	46012
25(*b*)	$K_2ZrSi_6O_{15}$	2.0	6.0	Dalyite	DAL	$P\bar{1}$	22323
26(*a*)	$Cs_2TiSi_6O_{15}$	2.0	6.0	Synthetic	TiSi-1	*C*2/*c*	84829
26(*b*)	$Cs_2ZrSi_6O_{15}$	2.0	6.0	Synthetic	ZiSi-3	*C*2/*m*	81440

Table 1 (continued)

No.	Compound	*w*	*q*	Mineral/synthetic	Structure type	Space group	Reference or collection code
27(*a*)	$CaSnSiO_5$	1.0	1.0	Malayaite	MAL	*A*2/*a*	81635
27(*b*)	$CaTiSiO_5$	1.0	1.0	Titanite-H	TIT-H	*A*2/*a*	9839
27(*c*)	$CaTiSiO_5$	1.0	1.0	Titanite-L	TIT-L	P 21/a	39870
28(*a*)	$Ca_3Zr_2(Si,Al,Fe)_3O_{12}$	1.5	1.5	Kimzeyite	KIM	$Ia\bar{3}d$	100258
28(*b*)	$Ca_3Sn_2SiGa_2O_{12}$	1.5	1.5	Synthetic	GAR§	$Ia\bar{3}d$	73815
29	$CaZrSi_2O_7$	1.0	2.0	Gittinsite	GIT	*C*2	203131
30(*a*)	$Ca_3SnSi_2O_9$	3.0	2.0	Synthetic	BAG	$P2_1/c$	80466
30(*b*)	$Ca_3ZrSi_2O_9$	3.0	2.0	Baghdadite	BAG	$P2_1/c$	79453
30(*c*)	$Na_2CaZrSi_2O_7(F,OH)_2$	3.0	2.0	Burpalite	BUR	$P2_1/a$	Bokij (1996)
31	$CaSnSi_3O_9(H_2O)_2$	1.0	3.0	Stokesite	STO	*Pnna*	34348
32	$Ca_2ZrSi_4O_{12}$	2.0	4.0	Synthetic	ZrSi-4	$P2_1/m$	73801
33	$CaZrSi_6O_{15}(H_2O)$	1.0	6.0	Armstrongite	ARM	*C*2	27752
34	$SrZrSi_2O_7$	1.0	2.0	Synthetic	ZrSi-5	$P2_1/c$	75272
35	$Sr_7ZrSi_6O_{21}$	7.0	6.0	Synthetic	ZrSi-6	$P\bar{1}$	75590
36	$BaZr_2Si_3O_{12}$	1.0	1.5	Langbeinite	LAN	$P2_13$	100420
37(*a*)	$BaSnSi_3O_9$	1.0	3.0	Pabstite	PAB	$P\bar{6}c2$	70104
37(*b*)	$BaTiSi_3O_9$	1.0	3.0	Benitoite	BEN	$P\bar{6}c2$	18100
37(*c*)	$BaZrSi_3O_9$	1.0	3.0	Bazirite	BAZ	$P\bar{6}c2$	70105
R = 7							
38(*a*)	$Na_2Ca_{10}Zr_2Y_2(Si_2O_7)_4(O,F)_8$	3.0	2.0	Hiortdahlite	HIO	$P\bar{1}$	68175
38(*b*)	$Na_6Ca_2Fe_4Zr_4(Si_2O_7)_4O,F)_8$	3.0	2.0	Lavenite	LAV	$P2_1/a$	100722
39	$Na_4MnTiZr_2(Si_2O_7)_2(O,F)_4$	1.0	1.0	Seidozerite	SEI	*P*2/*c*	30386
40	$Na_2Ca_4ZrNb(Si_2O_7)_2O_3F$	3.0	2.0	Woehlerite	WOE	$P2_1$	100158
R = 8–11							
41	$Na_5Ca_7Zr_2TiMn(Si_2O_7)_4(O,F)_8$	3.0	2.0	Rosenbuschite	ROS	$P\bar{1}$	22334
42(*a*)	$Na_{12}Ca_6Fe_3Zr_3Si_{24}O_{69}(OH)_3Cl$	7.0	8.0	Eudialyte	EUD	$R\bar{3}m$	23643
42(*b*)	$Na_{15}Ca_6Mn_3Zr_3NbSi_{25}O_{74}F_2(H_2O)_2$	8.33	8.33	Kentbrooksite	KEN	*R*3*m*	Johnsen *et al.* (1998)
42(*c*)	$Na_{15}Ca_3Mn_3Fe_3Zr_3NbSi_{25}O_{73}(O,OH, H_2O)_3(OH,Cl)_2$	8.33	8.33	Oneillite	ONE	*R*3	Johnsen, Gault *et al.* (1999)
42(*d*)	$Na_{12}Sr_3Ca_6Fe_3Zr_3(W,Nb)Si_{25}O_{73}(O,OH, H_2O)_3(OH,Cl)_2$	8.33	8.33	Khomyakovite	KHO	*R*3*m*	Johnsen, Grice & Gault (1999)

† Merwinite, $Ca_3MgSi_2O_8$ (CC = 26002). ‡ Phase obtained by the ion-exchange method. § Garnet, $Mg_3Al_2Si_3O_{12}$.

reaches 8–10 (Table 1). A high rank of atomic systems (R = 4–7) is also typical for the framework zeolites, but they are ordinarily classified by only framework-forming atoms T = {Al, Si} and O (R = 2), and in most of the models the rank is reduced to R = 1 when T atoms only are taken into consideration. The topological variety of zirconosilicate *MT* frameworks is also much greater than in any other chemical class of *MT* frameworks. Zr atoms in all *A*,*B*-zirconosilicates are allocated only in ZrO_6 octahedra; there are no direct connections between ZrO_6 octahedra, as a rule; they tend to be connected with *T* tetrahedra by vertices. In this respect they differ from Ti atoms, which are frequently allocated in condensed TiO_6-octahedra or in TiO_5-pyramids (for instance, in some Na-titanosilicates). It will be shown below that the *MT*-framework topological properties in all known K, Rb and Cs titanosilicates (Table 1) and in corresponding zirconosilicate are similar. Therefore, the main focus was framework zirconosilicates (all completely solved crystal structures were considered); the separate representatives of the numerous titanosilicate groups (for instance, Na titanosilicates) and other analogs were analyzed only in connection with their similarity to corresponding zirconosilicates.

The main investigation objectives were as follows:

(i) to show the possibility of constructing an unambiguous classification scheme for *MT* frameworks;

(ii) to derive topological types of *M* nodes and to compare them with the observed types in *MT* frameworks;

(iii) to determine the topological framework complexity (the number of topologically different *M* and *T* nodes);

(iv) to search for structural relationships between zirconosilicates and other *MT* frameworks;

(v) to illustrate the advantages and universality of the CS method application to the frameworks of different composition and topology.

To solve these problems we have tried to generalize the procedure of framework classification and to combine organically the SBU and CS methods as it is described in the next two parts.

3. Analysis and classification of *MT* frameworks using coordination sequences

With regard to aforesaid things to classify zirconosilicates we have developed a special variant of the general method of topological analysis of crystal structures using CS and '***reduced' graph*** concepts (Blatov, 2000). The isomorphism of framework-reduced graphs to be determined by comparing CS sets for all framework-forming atoms indicates mutual framework equivalence and specifies the corresponding compounds to be referred to the same ***topological type*** or ***topological family***. This approach assumes the formalization of crystal structure description. According to Blatov (2000) one can select the three main types of ***topological representations*** of a crystal structure:

(i) *As a net or subnet* when the following models of the crystal structure are to be used: (*a*) the structure is characterized by the whole net of existing chemical bonds (structure permits no simplification based, for instance, on the differentiation by bond types), or (*b*) a substructure with a subset of bonds separated in the crystal structure (in this case a decrease of the structure model rank is caused by removing one or several chemical types of atoms not belonging to the substructure together with all their bonds). For instance, the crystal structure of the matrix of NASICON superionic conductors with ideal composition $Na_4Zr_2Si_3O_{12}$ and statistically disordered Na-sublattices in the isomorphous analog $Na_3Zr_2Si_2PO_{12}$ may be presented as a net containing all atoms or only as a zirconosilicate framework where the atoms in the framework voids are to be forgotten.

(ii) *As a set of connected substructures*, which are to be considered as functionally equivalent. At the analysis of each substructure the atoms forming it are formally considered as complexing atoms and the remaining atoms assume to be referred to as ligands. The connectivity in each substructure is provided by contracting ligand atoms to complexing atoms, which results in a connected substructure of the complexing atoms with non-trivial topology. Let us emphasize that the procedure of contracting atoms, unlike their complete removal, keeps crystal structure bonds which form the edges of the connected substructure graph closing together (Figs. 1*a* and 1*b*). Such an approach appears to be especially fruitful in the analysis of atomic packings (Blatov, 2001). For instance, the NASICON structure may be considered as a framework consisting of cationic (with *M* and *T* atoms) and anionic (with O atoms) substructures.

(iii) *As a set of polyatomic (polyhedral) structural units* to be represented by the central atoms of coordination polyhedra. The topology of the system of their bonds with the surrounding atoms located in the polyhedron vertices is not to be considered and the surrounding atoms are to be contracted to the central atoms (Blatov, 2000). For example, the NASICON structure may be considered not as a framework of *T* tetrahedra and *M* octahedra but as a net consisting of four and six connected nodes without taking into account a way of joining together by common oxygen atoms (O nodes), *i.e.* without considering the topology of the O atoms surrounding the *T* and *M* nodes. At the analysis of topology of the channels containing mobile Na atoms, the representation can also be useful, when the *MT* framework is to be completely forgotten and the Na sublattice has to be classified as a three-dimensional net according to the results obtained that reflect the three-dimensional type of NASICON conductivity.

This general scheme covers all possible variants of crystal structure consideration and assumes computer automation of crystallochemical analysis (Blatov, 2000). A researcher has to choose one or another variant following crystallochemical reasons and his own view on the problem. Thus, in this study only the first type representations were considered to compare and classify zirconosilicates. Only framework-forming cations (Si, Zr, P, Al, *d*-metals) and anions O^{2-}, OH^- and F^- were included in the substructures, and $\{N_k\}$, $k = 1$–n, were calculated for all these atoms up to $n = 12$. This depth was accepted to be sufficient for the detection of the topological nonequivalence of framework atoms in zirconosilicates because the most similar nonequivalent sequences had a likeness up to $k = 10$. All remaining atoms in the compounds with any rank value (R = 3–11) were considered as off-framework and were ignored at the topological analysis.

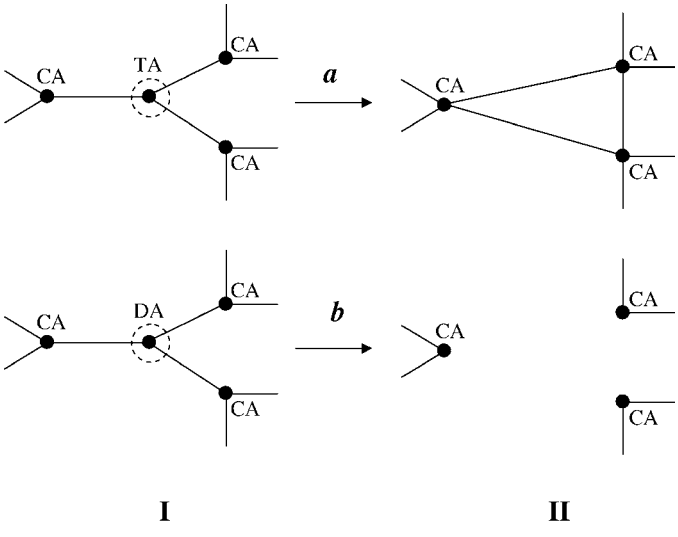

Figure 1
The procedures of transformation for graph fragment I to II by (*a*) contracting or (*b*) removing TA or DA atoms, respectively, in the sublattice of CA atoms. The nodes to be processed are marked by dashed circles.

4. Methods of analysis of *MT*-framework structural organization: cooperation of geometry and topology

4.1. Levels of *MT*-framework structural organization

The CS method, while yielding formal classification criteria, discerns no geometrical features of *MT*-framework structural organization. At the same time the *MT*-framework geometrical properties (in particular, relative sizes of coordination polyhedra and their components, crystal space symmetry) essentially influence the topological properties including CS values. In this part we shall consider a methodology of synthesis of *MT*-framework topological and geometrical properties, taking into account three levels of their structural organization: *atomic*, *polyhedral* and *suprapolyhedral*. In particular, this is the way to combine the SBU and CS methods on the same base.

At the *atomic* level the main classification parameters are the characteristics of point models of *MT* frameworks: the number and type of regular systems of points occupied by *M* and *T* atoms in fundamental regions of space groups, and the ratio of *T* and *M* nodes in a framework. In general, framework structures with the stoichiometric formulae $M_aT_bO_c$ can be generated by enumerating all integers *a* and *b* for hypothetical interacting electroneutral polyhedral particles

$$a[M(OH)_6] + b[T(OH)_4] \quad (1)$$

at their complete dehydration

$$[MO_{6/2}] + q[TO_{4/2}] = MT_qO_{3+2q}\ (q = b/a), \quad (2)$$

where the fractional values 6/2 and 4/2 indicate that all O nodes are shared between the PBU pairs *T*–O–*T*, *T*–O–*M* or *M*–O–*M*. In a ***topologically ideal MT-framework***, whose composition obeys the condition given in (2), all O atoms are bridging and the ratio of the number of *A* and *B* atoms to the number of *M* atoms (*w*, Table 1) can possess values within the range 1–2, which limits correspondence to the occupation of framework voids with only *B* or *A* atoms, respectively. The deviation of framework composition from (2) and exceeding the limits indicated by the *w* value justifies the appearance of terminal O atoms and appropriate framework gaps. Hereinafter we shall term such frameworks ***MT frameworks with O gaps***. The existence of gaps in an *MT* framework can result in a decrease in its dimensionality and the formation of two-dimensional *MT* layers, one-dimensional *MT* chains or isolated *MT* ensembles. It should be noted that the isolated *MT* ensembles are missing in zirconosilicates, but exist in Cs,Zr-molybdate, $Cs_8ZrMo_6O_{24}$.

At the *polyhedral* level it is necessary to identify at first MO_6 and TO_4 polyhedra and to state their role as framework-forming PBUs. Alkali (*A*) and alkaline-earth (*B*) atoms assume the occupation of framework voids and their subnet topology is not ordinarily studied. It is the stage when a compound is to be referred to the class of *MT*-framework zirconosilicates.

At the *suprapolyhedral* level the *MT* framework is to be described as a connected *MT*O substructure (*MT* framework with considering O atoms). At this level the framework atoms should be classified by CSs and SBUs or similar oligomeric structural units should be unambiguously selected, which consist of several PBUs and are ***suprapolyhedral invariants*** of the crystal structure. Hereinafter the following algorithm of hierarchical constructing suprapolyhedral invariants was used.

4.1.1. First sublevel. For each MO_6 and TO_4 polyhedra in a unit cell, all immediately bonded *M* octahedra and *T* tetrahedra are to be treated. In *MT* frameworks three compositions are possible of suprapolyhedral invariants to be constructed:

$$[MO_6]\text{–}[MO_6]_i, [TO_4]_j,\ i + j = 6;$$
$$[TO_4]\text{–}[MO_6]_i, [TO_4]_j,\ \ i + j = 4;$$
$$[TO_4]\text{–}[TO_4]_j,\ \ j = 0\text{–}4.$$

Thus, at the first sublevel suprapolyhedral invariants are represented by ***polyhedral microensembles*** (PME) constructed on the base of *M* or *T* nodes, and their view is determined unambiguously. This new term is introduced rather than SBU to emphasize that the procedure of PME construction differs from all known principles of SBU selection. After constructing PMEs and determination of topological characteristics of *M* and *T* nodes in a three-dimensional net, it is essential to search for their nonequivalence, as two crystallographically nonequivalent *M* or *T* nodes can be topologically symmetric, which is evident, in particular, in the equality of $\{N_k\}$. It is very important to query in the classification of framework zirconosilicates with CSs the minimum amount of topologically different *M* or *T* nodes from all the frameworks considered can be constructed, and what amount of CSs for what types of nodes is required for unambiguous identification of a framework. Thus, at this sublevel the set of CSs for all or part of the substructure atoms in a framework representation becomes the most important classification criterion.

4.1.2. Second and higher sublevels. For each PME of the first sublevel (PME-1) all PBUs are to be considered, which are connected with *M* and *T* polyhedra of PME-1. As a result a PME of the second sublevel (PME-2) is formed. More complex PMEs of the third, fourth *etc.* sublevels may be similarly generated from PMEs of the lower sublevels. Hereinafter we do not go beyond the first sublevel of the structural–topological analysis and consider only PMEs-1, the sublevel number for which will further be omitted for brevity.

PMEs visualize immediately CSs with $\{N_k\}$, $k = 1$–n, for *M* and *T* nodes and reflect the bond topology for crystal-forming *MT* precursors and their space correlations depending on the depth of calculation (Table 2). The geometrical model of layer-by-layer growth of the framework structure from *MT* precursors is close to the crystal chemical model of atomic interactions proposed by Aslanov (1988), but differs from it by the strict consideration of complex topology of an atomic net. It is convenient during classification to take on *M* nodes to be PME central atoms because (*a*) the number of these nodes is minimum in framework in comparison with *T* and O nodes, and (*b*) they have greater connectivity than the nodes of other types [in particular, *T* nodes which form $T(T + M)_4$ clusters] and therefore are characterized by more manifold topological structure. Hence, at the classification of zirconosilicates and their analogs the CSs of *M* nodes take on special significance.

4.2. Polyhedral microensembles MT_6: topological classification and hierarchy

Let us consider the topological properties of the PME MT_6 consisting of an *M*-octahedron (central polyhedron), all O vertices of which are divided with six *T* tetrahedra; the PME topology and CSs of framework atoms are mainly determined by the PBU geometrical parameters. Namely, the location of *T* tetrahedra on the surface of the *M* octahedron depends on the minimum distances between its O atoms (2.6–2.7 Å) and on small inclinations and rotations of *T* tetrahedra, allowing them to interact with each other forming additional *T*–O–*T* connections. However, the total number of combinatorially different variants of such a binding of *T* tetrahedra is rather limited in comparison with the number of variants possible for six isolated *T* tetrahedra, which are not connected with each other. The maximum degree of their condensation is sterically limited by construction of *only* two triplets of *T* tetrahedra. Each of the triplets can separately form its own types of combinations of *T*-tetrahedra with each other. Thus, the total number of solutions for MT_6 clusters will be equal to the number of possible combinations of TO_4 orthogroups with

Table 2
Alternation of coordination sphere compositions for the atoms forming an *MT* framework.

Framework-forming atom type	Atoms forming *k*th coordination sphere				
	$k = 1$	$k = 2$	$k = 3$	$k = 4$	$k = 5$
M	O	*M* and/or *T*	O	*M* and/or *T*	O
T	O	*M* and/or *T*	O	*M* and/or *T*	O
O	*M* and/or *T*	O	*M* and/or *T*	O	*M* and/or *T*

T_2O_7 diorthogroups and with triorthogroups in the form of T_3O_{10} chains or T_3O_9 rings. The combinatorial–topological problem of constructing all topologically different MT_6 blocks has a strict solution, which is to be considered next.

Let us introduce the following conventional signs for the topological description of binding *T* tetrahedra into MT_6-PMEs:

(i) p_i is a local connective index for *T* tetrahedra in the MT_6 ensemble equal to 0 (a free tetrahedron), 1 (a T_2O_7 diorthogroup) or 2 (when a tetrahedron forms two bonds with adjacent T_i; a triorthogroup is to be formed as a T_3O_{10} chain or T_3O_9 ring depending on p_i values of adjacent T_i tetrahedra);

(ii) $\{p_i\}$ is a set of six integers for each T_i in the MT_6 ensemble ordered by a decrease in characterization of the connectedness of all T_i on the MO_6 surface (for instance, {2, 1, 1, 1, 1, 0}, where the first three indices correspond to the triorthogroup, the next two indices conform to diorthogroup, and the last one to 'isolated' *T* tetrahedron);

(iii) MT_6 *isomers* are topologically different representations of MT_6 ensembles with the same $\{p_i\}$ set;

(iv) $P_l = \sum_{i=1}^{l} p_i$ is a cumulative index for *l T* tetrahedra in a PME (for an MT_6 ensemble $l = 6$) equal to the total number of O atoms of all *T* tetrahedra shared with adjacent *T* tetrahedra (without considering six O atoms of *T*-tetrahedra connected with the central *M* octahedron).

At the modelling of the cluster structures with graph theory the adjacent matrices are ordinarily used (Christofides, 1975). The simplest adjacent matrix *M*1 for the graph with three vertices ($l = 3$) is given as

$$M1 = \begin{pmatrix} T_i & 1 & 2 & 3 & p_i \\ 1 & 0 & a & b & a+b \\ 2 & a & 0 & c & a+c \\ 3 & b & c & 0 & b+c \\ p_i & a+b & a+c & b+c & P_3 = \Sigma p_i \end{pmatrix}.$$

For the T_3O_{10} chain or T_3O_9 ring clusters, the adjacent matrices may be written as *M*2 or *M*3, respectively.

$$M2 = \begin{pmatrix} T_i & 1 & 2 & 3 & p_i \\ 1 & 0 & 1 & 0 & 1 \\ 2 & 1 & 0 & 1 & 2 \\ 3 & 0 & 1 & 0 & 1 \\ p_i & 1 & 2 & 1 & P_3 = 4 \end{pmatrix}$$

$$M3 = \begin{pmatrix} T_i & 1 & 2 & 3 & p_i \\ 1 & 0 & 1 & 1 & 2 \\ 2 & 1 & 0 & 1 & 2 \\ 3 & 1 & 1 & 0 & 2 \\ p_i & 2 & 2 & 2 & P_3 = 6 \end{pmatrix},$$

$p_i = \{2, 1, 1\}$

$p_i = \{2, 2, 2\}$.

Merging the adjacent matrices corresponding to possible *T*–*T* combinations of diorthogroups (2×2 matrices) or triorthogroups (3×3 matrices) with isolated tetrahedra one can construct 12 different adjacent matrices describing combinatorially different MT_6 ensembles (Table 3, Fig. 2). The types C-1 and C-2 are MT_6 isomers; for them the allocation of two isolated *T* tetrahedra in the MT_6 block is possible both in *trans* and in *cis* positions. The octahedrally modified A and C ensembles are given in Table 3; they were found only in the frameworks MTO_5 and denoted as isomers A-1*M*, A-2*M* and C-1*M*. Thus, two forms derived from type A (A-1*M* and A-2*M*) reflect the substitution of two isolated *T* tetrahedra in the MT_6 block with two isolated *M* octahedra in *trans* and *cis* positions, respectively, and the isomer C-1*M* can be

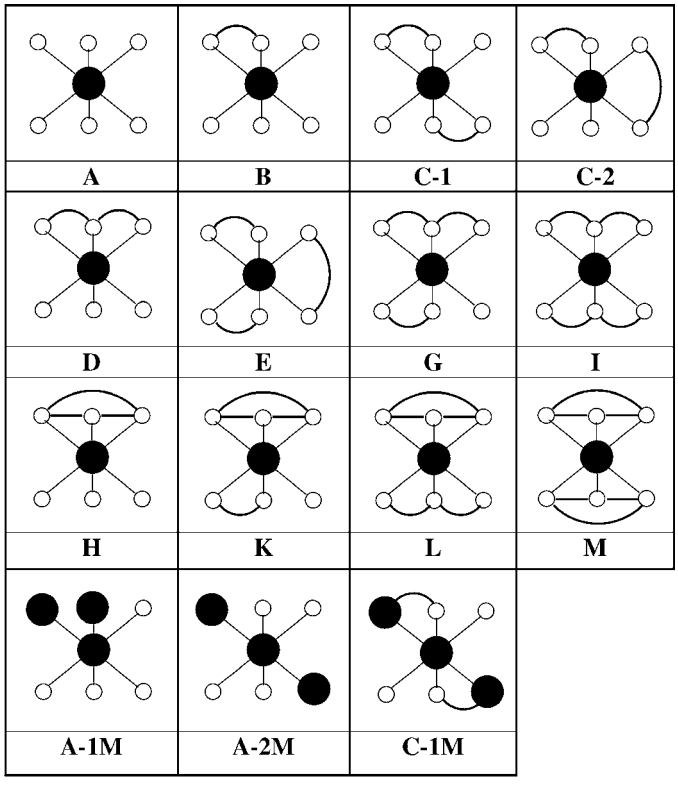

Figure 2
12 types of MT_6 ensembles and three types of $M(T_4M_2)$ ensembles (see Table 3). Black and white circles designate *M* and *T* atoms, respectively. O atoms are not shown.

Table 3
Topological characteristics and classification of MT_6 ensembles by coordination sequences of M atoms and connective indices of T tetrahedra.

No. and type refer to PME MT_6 with identical adjacent matrices combined into one type. N_k for k: coordination sequences are given with all PME atoms. $N_{1+}N_3$ represents the total number of O atoms in PME. The p_i values corresponding to the same T cluster are enclosed in square brackets.

			N_k for k						
No.	PME type	PME MT_6	1	2	3	$N_{1+}N_3$	$\{p_i\}$	P_6	Example
1(*a*)	A-1	$M(TO_4)_6$	6	6	18	24	000000	0	$Na_4Zr_2Si_3O_{12}$
1(*b*)	A-1M	*trans*-$M(TO_4)_4(MO_6)_2$	6	6	22	28	000000	0	$Na_2TiSi_4O_{11}$
1(*c*)	A-2M	*cis*-$M(TO_4)_4(MO_6)_2$	6	6	22	28	000000	0	Na_2ZrSiO_5
2	B	$M(T_2O_7)(TO_4)_4$	6	6	17	23	[11][0000]	2	$Na_4Sn_2Si_5O_{16}(H_2O)$
3(*a*)	C-1	*trans*-$M(T_2O_7)_2(TO_4)_2$	6	6	16	22	[11][0][11][0]	4	$Cs_2ZrSi_6O_{15}$
3(*b*)	C-1M	*trans*-$M(MTO_9)_2(TO_4)_2$	6	6	20	26	[11][11][00]	4	$CaTiSiO_5$
4	C-2	*cis*-$M(T_2O_7)_2(TO_4)_2$	6	6	16	22	[11][11][00]	4	$Na_2CaZr_2Si_{10}O_{26}(H_2O)_3$
5	D	$M(T_3O_{10})(TO_4)_3$	6	6	16	22	[211][000]	4	Not found
6	E	$M(T_2O_7)_3$	6	6	15	21	[11][11][11]	6	$Na_2ZrSi_3O_9(H_2O)_3$
7	G	$M(T_3O_{10})(T_2O_7)(TO_4)$	6	6	15	21	[211][11][0]	6	$K_2ZrSi_3O_9(H_2O)$
8	H	$M(T_3O_9)(TO_4)_3$	6	6	15	21	[222][000]	6	Not found
9	I	$M(T_3O_{10})_2$†	6	6	14	20	[211][211]	8	Not found
10	K	$M(T_3O_9)(T_2O_7)(TO_4)$	6	6	14	20	[222][11][0]	8	Not found
11	L	$M(T_3O_{10})(T_3O_9)$	6	6	13	19	[222][211]	10	Not found
12	*M*	$M(T_3O_9)_2$	6	6	12	18	[222][222]	12	Not found

† There can exist two MT_6 isomers with the local symmetries $\bar{1}$ and m.

Table 4
Distribution of 93 *MT* frameworks depending on the nature of the *M* atoms and the nature of the compound.

M atom	Silicates	Germanates	Minerals	Synthetic phases	Total
Zr	58	2	43	17	60
Sn	12	1	4	9	13
Ti	16	–	12	4	16
Si	4	–	–	4	4
Total	90	3	71 + 4	34	93

constructed by substitution of two diorthogroups with two MTO_9 groups, either of which consists of M octahedron and T tetrahedron. Other possible variants of substituting T nodes with M nodes do not occur in zirconosilicates and are not considered here.

5. Experimental

The comparative analysis of *MT*-framework zirconosilicates and the selection of topologically equivalent groups (families of *MT* frameworks) were carried out with the program package for multipurpose crystallochemical analysis *TOPOS*3.2 (Blatov *et al.*, 2000). The hierarchical analysis procedure included the following stages:

(i) *Creation of a database with MT frameworks.* At this stage all chemically and crystallographically different compounds, whose structures were mainly solved within the anisotropy approximation, were taken from the ICSD (release of August 2000) containing the information on 171 zirconosilicates (with R = 3–10). In a number of cases the original structural papers not included in the ICSD were used (for example, Johnsen, Gault *et al.*, 1999; Johnsen, Grice & Gault, 1999; Johnsen & Grice, 1999) and the recent data for minerals were taken (Khomyakov, 1995; Bokij, 1981, 1992, 1996, 1998). If Zr and Si atoms were disordered the compounds were selected in which the occupation factors for these atoms were no less than 0.5. Incompletely determined crystal structures and compounds with errors in the experimental data found by the program package *TOPOS* were forgotten. Chemically and crystallographically the most complex zirconosilicates with high rank, R = 7–10, containing, as a rule, other atoms with octahedral coordination (V, Ti, Y, Fe, Mn) together with Zr atoms, were selected in a separate group. In addition, the structural data of some zirconosilicate analogs included in the ICSD were analyzed, namely 141 titanosilicates (R = 4–6) and 30 stannosilicates (R = 4–8). The final list of compounds was extended with four high-pressure Si phases, two zirconogermanates and one stannogermanate (R = 3 and 5). For all the compounds the primary classification at an atomic level of structure organization was performed to select potential framework structures with the values of parameters w and q specified above. A complete list of 94 compounds (with $ZrSiO_4$) to be investigated is given in Table 1. The distribution

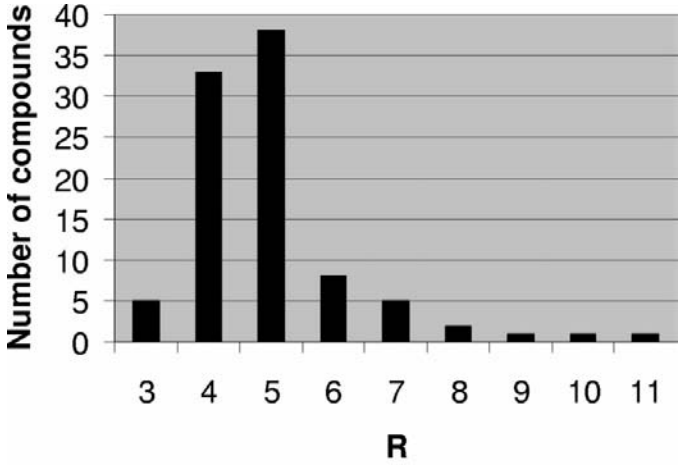

Figure 3
Distribution of *MT* frameworks depending on rank values.

Table 5
Homomorphic mapping between the sets of framework-forming atoms in $Na_6CaZr(Si_6O_{18})$ (I) and $Na_2ZrSi_6O_{15}(H_2O)_3(NaOH)_{05}$ (II).

Atoms are numbered according to the authors.

I	II	N_1	N_2	N_3	N_4	N_5	N_6	N_7	N_8	N_9	N_{10}	N_{11}	N_{12}
O1	O2,5,6	1	3	3	11	9	31	21	64	36	109	53	152
O2	O1,9,10	2	8	7	21	14	44	25	80	47	133	66	193
O3,4	O3,4,7,8	2	6	4	16	14	44	28	84	44	126	62	184
Si1	Si1,2,3	4	3	11	9	31	21	64	36	109	53	152	78
Zr1	Zr1	6	6	18	12	36	18	60	36	108	60	174	78

of 93 compounds (without non-*MT*-framework $ZrSiO_4$) depending on the nature of *M* atoms is given in Table 4, which refers the *MT*-frameworks to 60 Zr-, 16 Ti-, 13 Sn- and 4 Si-containing phases. The distribution of all phases depending on rank values R = 3–11 is shown in Fig. 3. Let us emphasize the following features of the distribution: (*a*) approximately equal amounts of phases with R = 4 and 5; (*b*) a sharp decrease in the number of structure types with an increase in chemical complexity for the phases with $R \geq 6$; only two structure types were detected at R = 8–11 (ROS and EUD). Of 60 Zr-containing phases 43 compounds are minerals, seven phases are synthetic analogs of minerals: LOV, MRW (two phases), ZEK and three phases obtained by ion exchange of K atoms with Na and Cs atoms in the UMB framework. Ten compounds with q = 1.0, 1.5, 2.0, 2.5, 4.0 and 6.0 are synthetic Zr phases, which have not been detected in nature and contain Na, Ca or Sr atoms. Among them there are six silicates, one germanate and three NASICON phases (this name is accepted for *synthetic phases* in the crystal chemistry of superionic conductors). Note that the compounds with q = 1–2.5, such as Na_2ZrSiO_5, $Na_4Zr_2Si_3O_{12}$ (NASICON), $Na_3HZrSi_2O_8$ and $Na_4Zr_2Si_5O_{16}(H_2O)$ (Ilyushin *et al.*, 1983) are missing among minerals of the Na,Zr-silicate series. The analysis of distribution of zirconosilicates and their analogs depending on the nature of *A* and *B* atoms shows that, as in zeolite systems, the greatest parts of phases with *A* or *B* atoms are composed of Na- or Ca-containing silicates, respectively; two phases with *B* = Sr are merely known for Zr silicates.

(ii) *Calculation of adjacent matrices of reduced graphs and PBU selection* for each crystal structure with the program *AutoCN*. At this stage, according to Blatov *et al.* (2000), only strong cation–anion contacts are to be treated for the 'major' faces of the atomic Voronoi–Dirichlet polyhedra with the solid angles $\Omega > 5\%$ of the total solid-angle 4π steradian. Note that a 'major' face of a Voronoi–Dirichlet polyhedron intersects a segment between contacting atoms and the point of intersection can often be considered (Blatov & Serezhkin, 2000) as an analog of the (3, −1) saddle point in the vector field of electronic density gradient, which indicates the existence of chemical bond between the atoms (Bader, 1990). To calculate adjacent matrices with the method of Blatov & Serezhkin (2000), the Slater system of atomic radii was used. At this stage it was revealed that the only exception among zirconosilicates with octahedral coordination of Zr atoms is zircon, which can be formally considered as an alkali-free zirconosilicate with R = 3 containing PBUs in the form of trigonal dodecahedra MO_8 and tetrahedra TO_4. Zircon topology is not appropriate to classify *MT* frameworks and is not considered here.

(iii) *Calculation of* $\{N_k\}$ for only framework-forming atoms in each crystal structure with the program *IsoTest* (Blatov, 2000, 2001), which was specially developed for the calculation of such representations only. At this stage the reduced graph of the structure is to be narrowed up to the reduced graph of a framework and all off-framework atoms and groups are to be forgotten. Owing to such optimized algorithms this, the most laborious, calculation stage took up ∼4 h of IBM PC 366 MHz computer time.

(iv) *Comparing the topology of framework reduced graphs* within various numbers of coordination spheres (k = 1–12) with the modified program *IsoTest*. According to Blatov (2000), the reduced graphs of two frameworks to be compared are to be considered as isomorphic within n coordination spheres if there is an isomorphic mapping between the sets of their representations on the basis of homomorphism of the representation sets $\{N_k\}$, k = 1–n. Actually, as each representation corresponds to a subnet selected in the framework, this isomorphism indicates the possibility of specifying a bijection between all subnets and, consequently, between the frameworks as a whole. At the same time, when comparing two substructures it is necessary to consider the possibility of the existence of topological symmetry in connected *M* and *T* substructures between crystallographically non-equivalent atoms, expressed as the equality of their $\{N_k\}$ values and hence belonging to the same topological type (Blatov, 2000). Thus, the total numbers of $\{N_k\}$ sets in isomorphic connected *M* and *T* substructures can differ from each other, but the numbers of non-equivalent $\{N_k\}$ sets are equal, which indicates homomorphism between the $\{N_k\}$ sets. For instance, in crystal structures of $Na_6CaZrSi_6O_{18}$ (zirsinalite, CC = 200800)[3] and $Na_3H_5ZrSi_6O_{18}$ (lovozerite, CC = 20595) the *MT* frameworks are isomorphic to each other, although the first framework includes only four independent O atoms, one Si atom and one Zr atom, while for the second framework the appropriate numbers are equal to ten, three and one, respectively. At the same time, it is possible to find the homomorphic mapping between sets of atoms, as shown in Table 5. Moreover, chemically different atoms occupying the same crystal-

[3] CC is a compound Collection Code in the ICSD.

Table 6
Classification of *MT* frameworks by topological types according to the coordination sequences of *M* atoms.

					Coordination sequences N_k (k = 1–12)											
No.	Compound	Structure type	*M* atom	PME type	1	2	3	4	5	6	7	8	9	10	11	12
Topologically ideal *MT* frameworks																
1	$K_2ZrSi_3O_9(H_2O)$	UMB	Zr1	G	6	6	15	12	42	32	81	47	133	83	206	109
2	$K_2ZrSi_3O_9(H_2O)$	KOS	Zr1	E	6	6	15	12	42	35	86	44	129	94	225	108
3(*a*)	$Na_2ZrSi_3O_9(H_2O)_2$	GAI	Zr1	E	6	6	15	12	42	36	94	51	138	96	248	125
3(*b*)	$NaKZrSi_3O_9(H_2O)_2$	GEO	Zr1													
4(*a*)	$Na_2ZrSi_3O_9(H_2O)_3$	HIL	Zr1,2	E	6	6	15	12	42	36	93	50	132	90	231	120
4(*b*)	$BaZrSi_3O_9(H_2O)_{2.5}$	KOM	Zr1,2													
5	$Na_2CaZr_2Si_{10}O_{26}(H_2O)$	LEM	Zr1	C-2	6	6	16	10	28	24	66	40	110	68	160	90
6	$Na_2TiSi_4O_{11}(H_2O)_2$	PEN	Ti1	C-1	6	6	16	12	38	28	76	50	140	84	192	106
7	$Na_5Zr_2Si_6O_{18}Cl(H_2O)_2$	PET	Zr1	C-2	6	6	16	12	38	30	86	50	132	74	188	108
8	$CaSnSi_3O_9(H_2O)_2$	STO	Sn1	C-1	6	6	16	12	38	30	88	54	142	82	208	118
9	$K_2ZrSi_6O_{15}$	DAL	Zr1	C-1	6	6	16	14	38	28	84	56	128	78	208	120
10(*a*)	$Cs_2ZrSi_6O_{15}$	ZrSi-3	Zr1,2	C-1	6	6	16	14	38	30	84	60	138	80	212	118
10(*b*)	$Cs_2TiSi_6O_{15}$	TiSi-1	Ti1													
11	$Na_4Zr_2Si_5O_{16}(H_2O)$	ZrSi-2	Zr1	B	6	6	17	12	40	30	92	54	137	77	209	121
12	$Na_4Zr_2Ge_5O_{16}(H_2O)$	ZrGe-1	Zr1	B	6	6	17	12	40	30	92	55	140	77	208	120
13	$SrZrSi_2O_7$	ZrSi-5	Zr1	B	6	6	17	14	54	39	103	54	165	105	266	122
14(*a*)	$Na_2ZrSi_2O_7$	pKEL	Zr1	A-1	6	6	18	12	42	30	102	50	122	74	222	108
14(*b*)	$K_2ZrSi_2O_7$	KHI	Zr1													
14(*c*)	$NaZr(Si_2O_6OH)$	KEL	Zr1													
14(*e*)	$Na_2SiSi_2O_7$	PKEL	Si2													
15	$Ca_3Zr_2SiAl_2O_{12}$	GAR	Zr1	A-1	6	6	18	12	54	42	114	50	186	114	270	110
16	$Na_4Zr_2Si_3O_{12}$	NAS	Zr1	A-1	6	6	18	13	60	39	96	46	180	105	240	101
17	$BaZr_2Si_3O_{12}$	LAN	Zr1	A-1	6	6	18	13	60	39	96	48	192	111	252	109
			Zr2	A-1	6	6	18	13	60	39	96	48	192	108	240	109
18(*a*)	$K_2SiSi_3O_9$	WAD	Si1	A-1	6	6	18	14	36	24	102	62	132	78	198	98
18(*b*)	$K_2ZrSi_3O_9$	WAD	Zr1,2													
18(*c*)	$Na_2ZrSi_3O_9(H_2O)_2$	CAT	Zr1,2													
19	$BaZrSi_3O_9$	BAZ	Zr1													
20	$Na_2SiSi_3O_9$	SiSi-1	Si1,3	A-1	6	6	18	14	39	30	108	62	138	84	237	134
			Si2	A-1	6	6	18	14	42	36	114	62	144	84	234	128
21	$CaZrSi_6O_{15}(H_2O)_2$	ARM	Zr1	A-1	6	6	18	16	42	26	76	52	136	84	200	108
22	$Na_2ZrSi_6O_{15}(H_2O)_3$	ELP	Zr1	A-1	6	6	18	16	46	24	62	40	122	78	206	114
23	$Na_2ZrSi_4O_{11}$	VLA	Zr1	A-1	6	6	18	16	54	32	90	60	170	90	226	126
24	$CaZrSi_2O_7$	GIT	Zr1	A-1	6	6	18	16	60	44	122	62	182	116	300	140
25	$NaLiZrSi_6O_{15}$	ZEK	Zr1	A-1	6	6	18	18	54	28	70	44	130	82	218	124
26	$KLi_3Zr_2Si_{12}O_{30}$	SOG	Zr1	A-1	6	6	18	18	54	29	72	42	120	75	210	122
27	$CaTiSiO_5$	TIT	Ti1	C-1M	6	6	20	16	60	40	116	64	206	104	280	144
28	$BaNa_2Ti_2Si_4O_{14}$	BAT	Ti1,2	A-1M	6	6	22	16	50	32	102	56	162	86	234	122
29	Na_2ZrSiO_5	ZrSi-1	Zr1,2	A-2M	6	6	22	17	60	39	127	71	202	100	307	155
30	$Na_2TiSi_4O_{11}$	NAR	Ti1	A-1M	6	6	22	18	54	34	94	54	150	86	230	126
MT-frameworks with gaps																
1	$Sr_7ZrSi_6O_{21}$	ZrSi-6	Zr1	A-1	6	6	18	6	18	6	30	30	90	30	90	18
2	$Na_3HZrSi_2O_8$†	MRW	Zr1	A-1	6	6	18	6	24	18	48	12	42	30	78	18
3	$Na_4ZrH_4Si_6O_{18}$	TER	Zr1	A-1	6	6	18	12	34	20	68	50	152	76	206	108
4(*a*)	$Na_8ZrSi_6O_{18}$	LOV	Zr1	A-1	6	6	18	12	36	18	60	36	108	60	174	78
4(*b*)	$Na_6CaZrSi_6O_{18}$	ZRS	Zr1													
4(*c*)	$Na_8SiSi_6O_{18}$	LOV	Si1													
5	$Ca_2ZrSi_4O_{12}$	ZrSi-4	Zr1	A-1	6	6	18	14	44	24	78	50	150	82	212	102
MT-condensed frameworks																
1	$Ca_3ZrSi_2O_9$	BAG	Zr1	*sp*-10‡	6	4	13	8	28	15	59	29	96	46	150	61

† Two-dimensional *MT* layers. ‡ See Fig. 9.

lographic position can belong to the same topological type. The most typical case is mixed frameworks containing *M* and/or *T* atoms of different nature, for example, Zr and Sc or Si and P atoms in the compounds of the NASICON structure type. Since during the analysis of the framework topology such atoms are considered together, a search for their 'grey' isomorphism is to be performed during a comparison of their representation sets, when the nature ('colour') of framework atoms is not taken into account.

(v) PME identification was carried out for all different *M* and *T* nodes in *MT* frameworks of the same topological type by means of comparing N_k values for k = 1–3 with N_k values characterizing12 PME types found theoretically (Table 3). Then *M* clusters were visualized to detect the types of topological MT_6 isomers. The sets of visualized *M*- and *T*-PMEs, as well as CS values for *M*- and *T*-nodes are the most important structural characteristics of zirconosilicates and their analogs in the Atlas of *MT*-frameworks to be produced in the near future.

Table 7
Topological types of *MT* frameworks arranged by the coordination sequences of *T* atoms.

The representatives of the topological families indicated in Table 6 are merely given. *MT* frameworks with the same numbers of topological types of *T* nodes are arranged by an increase of N_k values (or of their sum in the case of several topological types of *T* nodes) for a given *k*.

			Coordination sequences N_k (k = 1–12)											
No.	Topological type	*T* atom	1	2	3	4	5	6	7	8	9	10	11	12
One topological sort of *T* node														
1	ZrSi-6†	Si1,2,3	4	2	8	6	20	10	30	10	40	30	100	46
2	LOV†	Si1	4	3	11	9	31	21	64	36	109	53	152	78
3	MRW†	Si1,2	4	3	15	12	33	9	33	24	63	15	51	36
4	HIL	Si1	4	4	14	12	34	28	86	56	140	82	214	120
5	SOG	Si1	4	4	14	12	40	29	84	53	138	78	194	105
6	NAR	Si1	4	4	14	12	42	28	84	52	144	82	218	118
7	CAT	Si1	4	4	15	12	42	30	72	44	142	80	217	120
8	BAZ	Si1	4	4	15	12	42	30	74	50	150	76	207	120
9	BAT	Si1,2	4	4	16	13	48	30	92	53	156	84	240	122
10	KHI	Si1,2	4	4	18	15	48	27	78	49	156	76	198	108
11	GIT	Si1	4	4	18	17	50	36	118	72	189	100	288	161
12	TIT	Si1	4	4	19	16	52	38	127	64	182	102	309	144
13	GAR	Si1	4	4	20	16	44	28	124	74	172	76	284	162
14	NAS	Si1	4	4	20	16	44	26	112	66	152	70	268	150
15	LAN	Si1	4	4	20	16	44	26	112	66	152	73	286	156
16	ZrSi-1	Si1,2	4	4	20	17	58	37	112	63	208	112	305	143
Two topological types of *T* nodes														
1	BAG‡	Si1	4	3	13	7	25	15	50	25	93	42	142	63
		Si2	4	2	8	5	20	13	45	22	75	36	130	57
2	ZrSi-4†	Si1	4	3	11	9	32	24	73	43	125	68	199	106
		Si2	4	4	16	13	43	29	84	45	130	69	202	110
3	ZrSi-3	Si1,2,6	4	4	13	12	34	27	76	53	133	83	201	118
		Si3,4,5	4	4	14	14	39	28	75	53	137	84	201	119
4	ELP	Si1,2	4	4	14	11	36	27	78	48	122	67	170	96
		Si3	4	4	14	11	34	26	76	46	120	66	166	95
5	PEN	Si1	4	4	15	12	32	25	76	51	129	72	191	118
		Si2	4	4	13	11	34	25	71	46	119	72	193	115
6	UMB	Si1	4	4	14	12	34	26	81	51	127	79	204	107
		Si2,3	4	4	14	11	32	26	77	50	128	74	199	112
7	ZEK	Si1,3	4	4	14	12	40	30	88	55	142	79	196	107
		Si2	4	4	14	12	40	29	82	51	134	75	194	111
8	ARM	Si1,2,3,4	4	4	14	12	38	29	80	50	125	77	198	114
		Si5,6	4	4	14	13	38	27	75	49	131	78	189	111
9	PET	Si1	4	4	14	12	36	25	74	52	134	71	188	106
		Si2	4	4	15	13	39	27	74	49	135	76	195	108
10	STO	Si1	4	4	14	12	36	26	78	54	144	80	200	120
		Si2	4	4	15	13	39	28	78	52	140	81	211	119
11	VLA	Si1	4	4	16	14	44	31	92	53	146	87	238	128
		Si2	4	4	14	11	38	29	90	56	158	88	230	128
12	ZrSi-5	Si1	4	4	17	15	44	30	100	64	167	86	248	144
		Si2	4	4	17	15	44	31	102	63	164	86	254	147
Three topological types of *T* nodes														
1	TER†	Si1,6	4	2	8	8	26	19	56	36	112	63	179	90
		Si2,5	4	3	11	11	35	21	66	40	118	67	193	97
		Si3,4	4	4	14	10	34	24	70	41	122	66	193	105
2	LEM	Si1,4	4	4	13	11	33	22	59	40	106	65	165	94
		Si2,3	4	4	15	12	30	20	58	42	110	64	163	93
		Si5	4	4	12	10	32	23	62	40	110	67	154	86
3	DAL	Si1	4	4	14	14	42	29	76	52	134	82	203	114
		Si2	4	4	13	11	33	27	77	55	136	77	192	117
		Si3	4	4	13	11	33	27	75	52	135	80	196	115
4	KOS	Si1	4	4	14	12	34	26	80	55	139	80	207	116
		Si2	4	4	14	12	34	27	80	52	129	75	207	121
		Si3	4	4	14	12	34	26	80	55	135	77	212	123
5	GAI	Si1	4	4	14	12	34	28	86	55	137	84	222	126
		Si2	4	4	14	12	34	28	86	56	143	87	225	127
		Si3	4	4	14	12	34	28	85	54	134	79	215	130
6	ZrSi-2	Si1	4	4	14	12	38	28	90	54	140	76	198	112
		Si2	4	4	15	13	44	28	75	50	147	82	211	112
		Si3	4	4	18	15	42	27	78	50	148	88	225	112
7	ZrGe-1	Ge1	4	4	18	15	42	27	78	51	150	89	229	109
		Ge2	4	4	15	13	44	28	75	51	148	80	208	112
		Ge3	4	4	14	12	38	28	90	54	136	72	194	112

Table 7 (continued)

No.	Topological type	*T* atom	Coordination sequences N_k (k = 1–12)											
			1	2	3	4	5	6	7	8	9	10	11	12
8	SiSi-1	Si4,7,10	4	4	16	14	46	33	82	52	164	95	232	125
		Si5,8,11	4	4	16	14	46	32	86	56	156	90	240	128
		Si6,9,12	4	4	16	14	46	33	86	56	162	91	234	125

† *MT* framework woth O gaps. ‡ *MT* condensed framework.

6. Results and discussion

6.1. Classification of framework zirconosilicates and their analogs with *R* = 3–6 by coordination sequences of *M* nodes

The results of the analysis of 36 topological types of zirconosilicates and their analogs with R = 3–6 (Tables 7 and 8) allow one to conclude that the universal model of their structure is a three-dimensional periodic net containing nodes of two types (M and T) with the coordination numbers equal to six (octahedral nodes) or four (tetrahedral nodes). Such topologically ideal MT frameworks were revealed in 30 topological types. In six other cases, for $Na_3HZrSi_2O_8$ (MRW), $Na_8ZrSi_6O_{18}$ (LOV), $Ca_3ZrSi_2O_9$ (BAG), $Ca_2ZrSi_4O_{12}$ (ZrSi-4), $Sr_7ZrSi_6O_{21}$ (ZrSi-6) and $Na_4H_4ZrSi_6O_{18}$ (TER), MT frameworks contain O gaps owing to an increased abundance of A and B atoms.

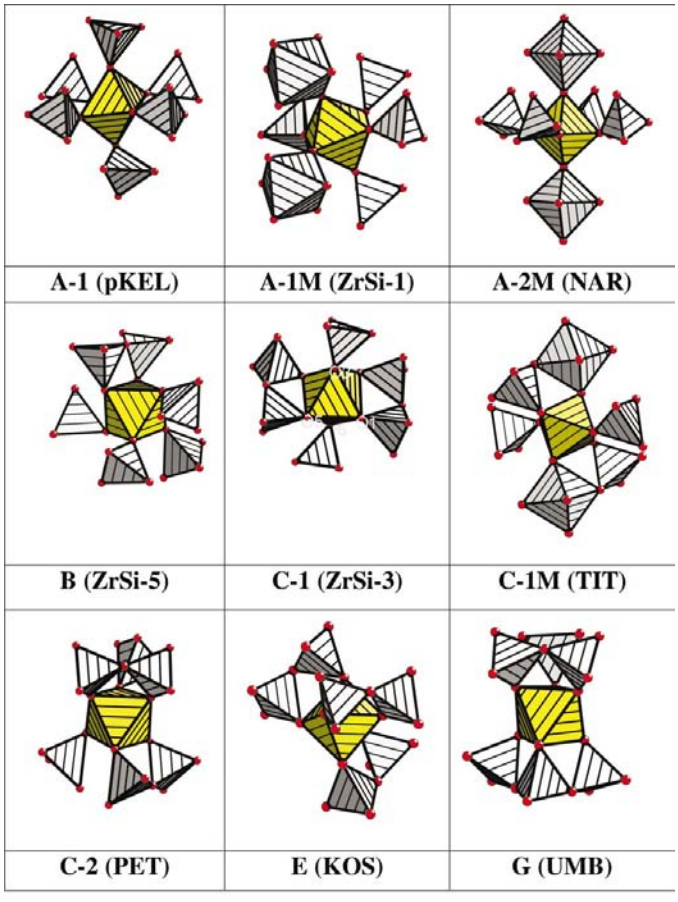

Figure 4
PME types for M nodes revealed in MT frameworks.

In all topological types PBUs are united only by vertices in the combinations T + T, T + M or M + M. A unique MT framework with edge condensation of Zr octahedra was detected in $Ca_3ZrSi_2O_9$ (BAG, R = 4, Table 1). This framework is characterized by M nodes with N_{1-3} = {6, 4, 13}, where the second topological index is not equal to six as in all MT frameworks (Table 6, Fig. 4), but caused by connecting only four PBUs with O atoms of the central M octahedron. In view of the edge condensation of M polyhedra and vertex condensation of three T tetrahedra with O atoms of the central M octahedron, its sixth vertex remains free (see §6.5). Such a type of O gap in M ensemble is unique. Its appearance causes the substitution of O atoms in Zr octahedra with OH groups or F atoms and simultaneous partial replacement of off-framework Ca atoms with Na atoms as in the crystal structure of $Na_2CaZrSi_2O_7(F,OH)_2$ (BUR).

The q parameter in (2) varies from 1 to 6 with the half step that conforms to varying MT-framework composition from MTO_5 to MT_6O_{15}. The arrangement of zirconosilicates and their analogs with eight observed q values is extremely irregular: the maximum numbers of representatives are 23, 19 and 16 for q = 3, 6 and 2, respectively. The only framework topological type is found for LEM (q = 5); in other cases the numbers of representatives are equal to 5 (for q = 1 and 4) or 4 (for q = 2.5). Thus, only three from 11 theoretically possible framework types [$M_2T_7O_{20}$ (q = 3.5), $M_2T_9O_{24}$ (q = 4.5) and $M_2T_{11}O_{28}$ (q = 5.5)] have not yet been discovered in the composition range from MTO_5 to MT_6O_{15}.

O atoms can have two different coordination types in MT frameworks: bridging (in T–O–T, M–O–T and rarely M–O–M groups) and terminal (in T–O and M–O groups). In Tables 7 and 8 MT frameworks with gaps containing terminal O atoms are considered separately. The values w = 8 and 7 are maximum for $Na_8ZrSi_6O_{18}$ and $Sr_7ZrSi_6O_{21}$ among the compounds with A and B atoms, respectively (Table 1). These compounds contain maximum numbers of 'abundant' O atoms in comparison with topologically ideal framework MT_6O_{15}.

The space symmetry data on crystal structures of zirconosilicates indicate that MT frameworks are characterized by the strict symmetry selection of M nodes: a unit cell contains one non-equivalent M atom, as a rule. The topological analysis of MT frameworks shows that in six of seven cases when the crystal structure comprises two crystallographic types of M nodes (no examples with a greater number of non-equivalent M atoms were detected), they are topologically the same (Table 6). The only exception is the crystal structure of $BaZr_2Si_3O_{12}$ (LAN; Masse & Durif, 1973), whose CSs were

Table 8
Coordination sequences of *M* nodes in *MT* frameworks with complex composition.

		Coordination sequences N_k (k = 1–12)											
Structure type	*M*(*T*) atom	1	2	3	4	5	6	7	8	9	10	11	12
MT frameworks with gaps													
SEI	Zr1	6	8	25	19	56	45	138	81	201	116	302	182
	Ti1	6	8	26	16	48	42	128	82	208	114	296	180
	Mn1	6	6	22	16	46	38	112	74	196	110	286	172
ROS	Zr1	6	6	18	11	37	21	71	34	99	60	190	94
	*M*1†	6	6	18	10	30	18	64	36	106	50	156	88
	*M*2†	6	4	12	8	30	24	84	44	118	56	168	76
WOE	Zr1	6	6	19	10	35	23	84	47	143	63	198	96
	Nb1	6	4	13	10	33	20	75	42	131	66	206	90
LAV-I	Zr1	6	8	25	17	51	43	133	79	201	111	283	173
	Fe1	6	7	24	18	51	41	123	77	199	111	287	170
LAV-II	Zr1	6	5	15	10	37	24	85	42	121	62	195	89
HIO	Zr1,Y1												
Two-dimensional *MT*-layers													
EUD	Zr1	6	6	18	12	34	12	36	20	58	30	80	26
ONE	Zr1	6	6	18	12	34	16	48	24	66	26	68	30
KEN	Zr1												

† $M1,2 = \frac{1}{2}$Mn + $\frac{1}{2}$Ti.

calculated using the data for the isotypic analog $K_2Mg_2(SO_4)_3$ [CC = 100420]. In this case the N_k values of two non-equivalent *M* atoms differ from each other starting only from the tenth coordination sphere!

We have performed a hierarchical classification of crystal structures of zirconosilicates on the basis of the topological model described here. The ordered CS sets for *M* nodes in all *MT* frameworks are given in Table 6. The data of Table 6 show that $n \geq 10$ is required for the identification of all framework-forming atoms in zirconosilicates and their analogs which is twice the value used by Meier & Moeck (1979) for the analysis of zeolite frameworks; however, it corresponds to the depth accepted in the *Atlas of Zeolites*. Actually, the cases when different CSs of *M* atoms remain identical up to the fifth coordination spheres are quite ordinary. Besides *M* atoms in the above-mentioned LAN structure, the high similarity is found for the pairs of topological types langbeinite–NASICON (up to $k = 8$), gaidonnayite–hilairite (up to $k = 7$), umbite–kostylevite (up to $k = 6$) *etc*.

In almost all zirconosilicates it is sufficient to specify CSs only for *M* atoms to identify a topological type. The single exception is the bazirite crystal structure. The CSs of Zr atoms in this structure are identical to those in wadeite and catapleite crystal structures, while their differences become apparent in CSs of *T* atoms starting from the seventh coordination sphere (Table 7). This structural feature may be referred to by the minerals indicated being the topological isomers constructed from the same structural units: triple rings [Si_3O_9] and isolated octahedra [ZrO_6] alternating along the hexagonal axis (Fig. 5). The *MT* chains [001] are geometrically and topologically equivalent in all three structures and represent the columns where each *M* octahedron is united by vertices with six isolated *T* tetrahedra. The *MT* layers (001) differ from each other only by rotations of triple rings; the rings [Si_3O_9] in bazirite lie under each other in pairs, while in wadeite and catapleite two ring triples are turned round each other. Such rotations cannot be topologically detected in a mixed *MT* structure, but they can be identified by the topological analysis of connected *T* substructures (Table 7).

In total, 73 *MT* frameworks with $R = 3$–11 are arranged in 21 families with the numbers of topologically equivalent representatives varying from two to 11 (Table 1). Note that the most numerous families LOV and CAT–WAD with 11 and 9 representatives, respectively, are characterized by different amounts of *A* and *B* atoms, different space groups and the number of occupied crystallographic orbits. In most cases the determination of the topological equivalence of their frameworks is not a trivial problem. On the whole, there are 41 topologically different *MT* frameworks and 20 types of *MT* frameworks are unique. Let us emphasize that in the crystal structures of $Na_8ZrSi_6O_{18}$, $Na_6CaZrSi_6O_{18}$, $Na_6MnTiSi_6O_{18}$ and $Na_6FeTiSi_6O_{18}$, belonging to the first (by population) LOV family, the Na, Ca, Mn and Fe atoms are allocated to the same crystallographic positions (on the threefold axes), which indicates their identical role as off-framework atoms in constructing these phases. The Zr phases with $R = 7$–11 considered in §6.5 are more complex crystallographically: in their crystal structures there may be atoms potentially playing the role of both framework-forming and off-framework, as in ROS and zirconosilicates of the EUD family where the determination of the structural function of Na, Ca, Fe, Mn, Nb, Zr, Si and O atoms becomes a non-trivial problem.

6.2. Local and global topological properties of *T* nodes in compounds with $R = 3$–6

Although the most efficient method of *MT*-framework systematization is the use of CSs of *M* nodes, it is of interest to consider the local and global topology of *T* nodes to clear up the differences between connected *M* and *T* substructures and the framework-forming role of corresponding suprapolyhedral *T* invariants. Let us emphasize that in this case the

notion 'global topology' is non-rigorous because the CS calculation was performed on a rather large (n = 12) but local part of the *MT* framework. At the same time the data obtained allow us to state that this depth of analysis is sufficient for topological identification of the framework as a whole.

In Table 7 the CSs for the compounds with R = 3–6 are given for all *T* nodes in 30 types of topologically ideal *MT* frameworks, in five types of *MT* frameworks with O gaps and in one *MT* framework with O gaps and edge condensation of *M* octahedra. Note that the presence of $N_2 < 4$ in CSs of *T* nodes shows unambiguously that six *MT* frameworks have gaps and the terminal O nodes connected with *T* atoms correspond to these gaps. For instance, in the crystal structure of TER *T* tetrahedra Si(1,6) (with $N_2 = 2$) and Si(2,5) (with $N_2 = 3$) have two and one terminal O atoms, respectively. In Table 7 all *MT* frameworks are arranged in three groups, depending on the number of topological sorts of *T* nodes. At the beginning of each group the frameworks are arranged by an increase in the topological indices and hence *MT* frameworks with gaps (three, two and one type of O gap in the first, second and third group, respectively) always lead the group lists.

Eleven out of 16 *MT* framework types contained in the first group are characterized by one crystallographic (and topological) type of *T* atom (Table 7). In other frameworks (ZrSi-1, ZrSi-6, KHI and BAT) and in two-dimensional *MT*-layer structure (MRW) non-equivalent *T* atoms are topologically the same, *i.e.* *T* substructures of these frameworks have non-trivial topological symmetry. Thus, 13 types of ideal *MT* frameworks and three *MT* frameworks with O gaps can be constructed from the same type of suprapolyhedral *T* invariant.

The geometrical models of 17 other topologically ideal *MT* frameworks of the second and third group are characterized by two, three, five, six and nine crystallographically different *T* nodes (Table 7). *T* subnets in ten *MT* frameworks with small (two and three) numbers of non-equivalent *T* nodes possess non-trivial topological symmetry. Seven *MT* frameworks with 3–9 non-equivalent *T* nodes have strong topological symmetry: the maximal number of topological sorts of *T* nodes does not exceed three. This phenomenon occurs not only in topologically ideal *MT* frameworks, but also in *MT* frameworks with gaps: in $Sr_7ZrSi_6O_{12}$ (ZrSi-6) and TER three and six crystallographically different *T* atoms fall into one and three topological sorts, respectively. In the BAG framework both *T* nodes possess a lower connectivity because of their N_{1-3} = {4, 2, 8} and {4, 3, 13}.

The PMEs of the first sublevel are visualized in Fig. 6 for some of the 54 topological types of *T* node in 30 topological types of ideal *MT* framework. All nine different N_{1-3} sets lie within the range {4, 4, 12}–{4, 4, 20} (Fig. 6) and the marginal N_{1-3} sets correspond to a central *T* tetrahedron connected with four isolated *T* tetrahedra or *M* octahedra, respectively. Moreover, three and two topological isomers are found for the *T* nodes {4, 4, 14} and {4, 4, 15}, respectively (Fig. 7). Thus, 12 PME topological types exist for nine different sets {4, 4, N_3}, whose frequencies are extremely irregular. For instance, PMEs with N_{1-3} = {4, 4, 12} and {4, 4, 19} are found only in LEM and TIT structures, respectively. Note that the *T* node {4, 4, 12} in LEM is a local structure fragment of any tetrahedral SiO_2 polymorph, *i.e.* it is the only example of all 12 detected PME types in which the *M*—O—*T* bonds are missing. It is the *T* node which is completely occupied by Al atoms in altisite $Na_3K_6Ti_2(Al_2Si_8O_{26})Cl_3$ [CC = 79853], a Ti analog of LEM.

The PME type, of the composition $T(3T + M)$ with N_{1-3} = {4, 4, 14} realised in 16 ideal *MT* frameworks, is the most typical for *T* nodes. It should be noted that the {4, 4, 20} set with the greatest possible N_3 value corresponds to the PME in which the central *T* tetrahedron is connected with only four isolated *M* octahedra, *i.e.* the frameworks with such *T* nodes may be automatically referred to the orthosilicate family. The zirconosilicates LEM, DAL, GAI, KOS and $Na_4Zr_2Si_5O_{16}(H_2O)$ are examples of topologically the most complex *MT* frameworks with three types of *T* nodes. Note a strong

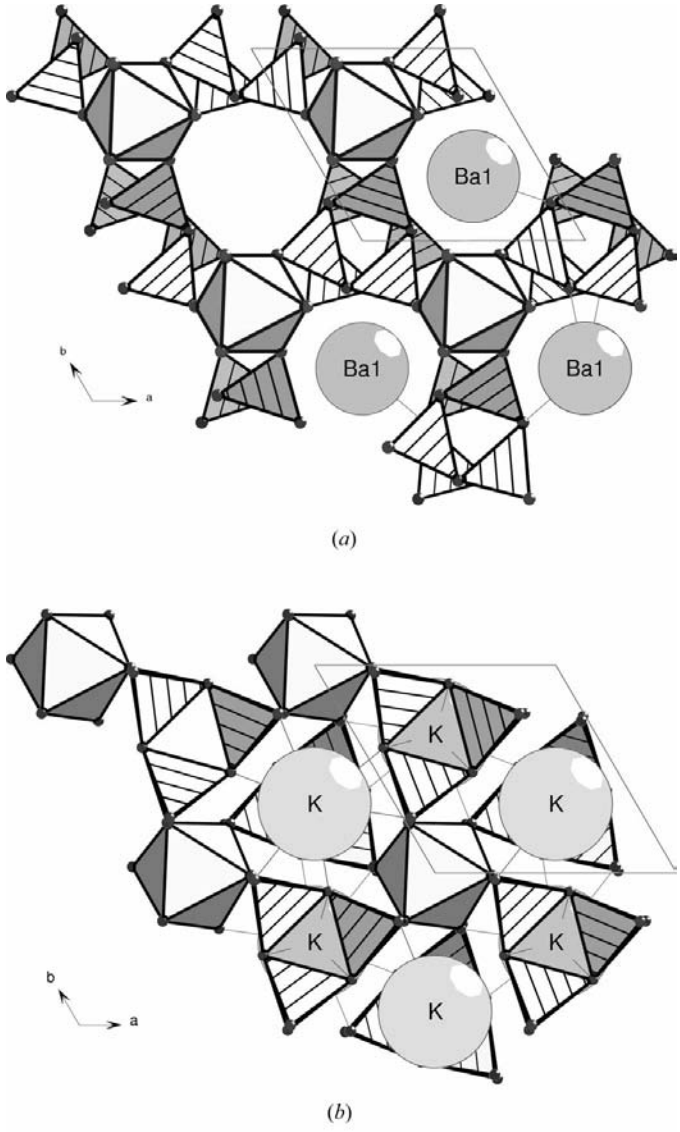

Figure 5
*XY*0 projections of the crystal structures of MT_3O_9 topological isomers: (*a*) bazirite; (*b*) wadeite.

topological similarity of *T* nodes in GAI and KOS: the differences between *all of them* are cleared up starting only from the sixth coordination sphere!

Thus, the maximum topological complexity of zirconosilicates conforms to their presence in frameworks of up to four topological types of node (one type of *M* node and three types of *T* node, the third group in Table 6).

6.3. Local topology of *M* nodes

Among 30 topological types of ideal *MT* frameworks nine types of *M* nodes are found, which are locally different within the first three coordination spheres (Tables 4 and 7; Fig. 4) which corresponds to PMEs of the first sublevel. All indicated types of *M* nodes are characterized by $N_{1-3} = \{6, 6, N_3\}$, where N_3 = 15, 16, 17, 18, 20 or 22. Chemical isomerism of the {6, 6, 15} nodes corresponding to $M(T_3O_{10})(T_2O_7)(TO_4)$ or $M(T_2O_7)_3$ ensembles, and geometrical *cis*/*trans* isomerism in the arrangement of TO_4 and MO_6 polyhedra for the nodes {6, 6, 16} and {6, 6, 22}, respectively, are considered (Table 6). All zirconosilicates can be arranged in three groups depending on N_3 values:

(i) *First PME group* with N_3 = 15, 16 or 17. Five of six types of MT_6 ensembles detected in *MT* frameworks occur in 16 phases referring to 13 topological types (Table 3). The PME $M(T_2O_7)_2(TO_4)_2$ with TO_4 tetrahedra in *trans* positions (C-1 type), the PME $M(T_2O_7)_3$ with three T_2O_7 diorthogroups (E type) and the PME $M(T_2O_7)(TO_4)_4$ with one diorthogroup (B type) are realised in five, five and three phases, respectively. The C-2 type with *cis* positions of TO_4 groups is revealed for the PME $M(T_2O_7)(TO_4)_4$ in the PET and LEM frameworks. Only one example of the PME $M(T_3O_9)(T_2O_7)(TO_4)$ with three different *T* groups (G type) is found in the UMB framework. Most of the frameworks in this group (12 of 16) are water-containing phases with a low density of *M* nodes (q = 3–6). Anhydrous phases (DAL and ZS-1) contain the largest alkali and alkaline-earth atoms (K, Cs and Sr).

(ii) *Second PME group* with N_3 = 18. All 19 compounds of this group falling in 13 topological types comprise the same PME-type $M(TO_4)_6$ (A) with six isolated *T* tetrahedra. Only three types of *MT* frameworks (CAT, ARM and ELP) contain water molecules and medium-sized Na and Ca cations in the framework voids at q = 3 or 6. This group also covers the most frequent among *M* phosphate and *M* sulfate crystal structures with the GAR, LAN and NAS frameworks. It is completed with ZEK and SOG frameworks in Li-containing phases.

(iii) *Third PME group* with N_3 = 20 or 22. Three of four phases in this group are titanosilicates. This group contains two topological types of the frameworks MTO_5, MT_2O_7 and MT_4O_{11}. The *M* modified nodes in PMEs can be obtained from the canonical PME of MT_6 composition by the replacement $2T \Rightarrow 2M$. In the TIT framework they have the composition $M(TMO_9)_2(TO_4)_2$ (C-1*M* type) with two TMO_9 groups of *M* + *T* polyhedra united by vertices. The *A* type $M(TO_4)_4(MO_6)_2$ with isolated polyhedra occurs in two

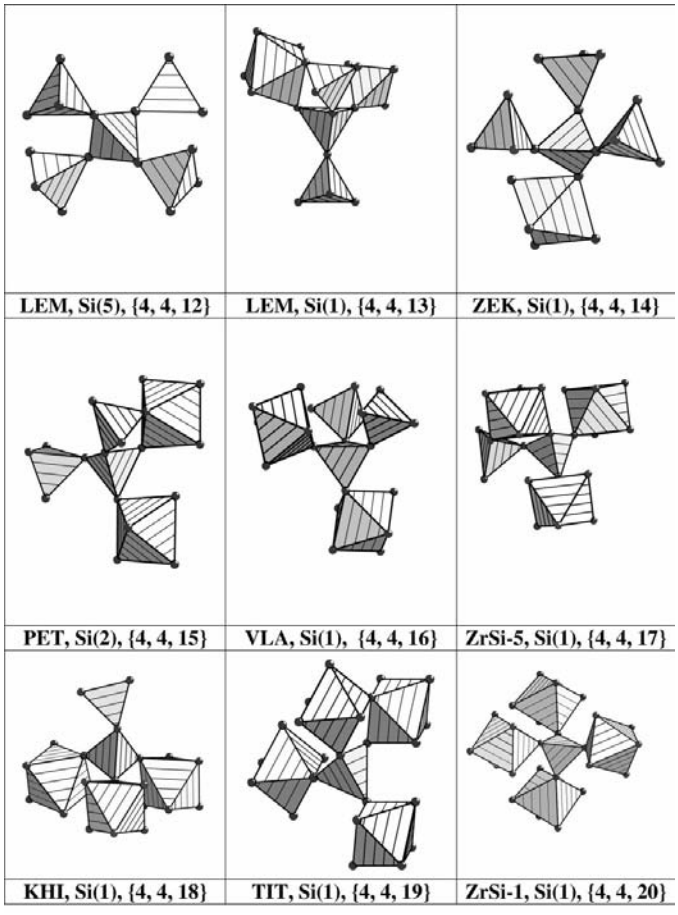

Figure 6
Some PME types for *T* nodes revealed in *MT* frameworks. The *T*-atom name and coordination sequence $\{N_k\}$, k = 1–3, are specified for each *T* node.

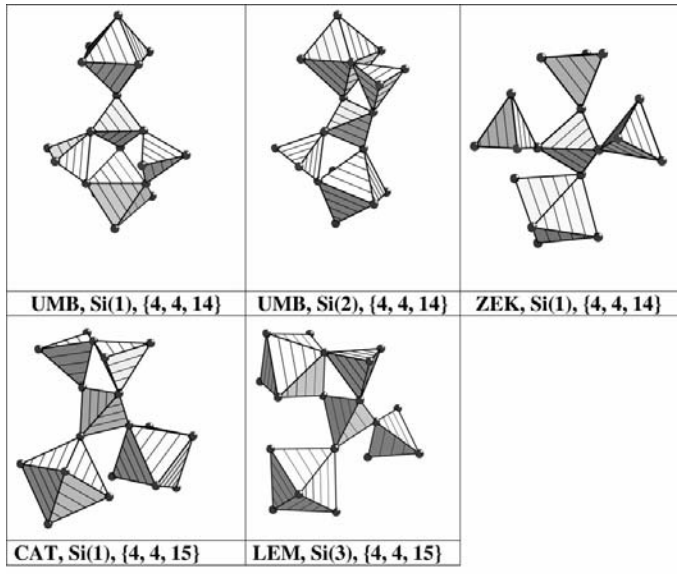

Figure 7
Topologically different PME isomers for the *T* nodes {4, 4, 14} and {4, 4, 15} revealed in *MT* frameworks.

variants (Table 3): with MO_6 octahedra in *trans* positions (the type A-2*M* in the titanosilicates with the NAR and BAT frameworks) and in *cis* positions (the type A-2*M* in the ZrSi-1 zirconosilicate).

6.4. Topological features of some *MT* framework types

As was mentioned above, the automation of all stages of *MT*-framework topological analysis allows one to use the CS sets for comparing and searching for structural relations with any other compounds, including ones of other rank, for example, with the more simple (in composition) ternary $A_xB_yC_z$ compounds, according to the principles described by Blatov (2000). The search in the earlier generated database containing more than 5000 topological types for more than 19 000 ternary compounds (including the phases with non-localized H atoms) has shown that they are completely analogous to *MT* frameworks only in three cases:

(i) The NAS framework occurs in the phases $M_2(SO_4)_3$ (*M* = Al, Ga, Fe, Cr, In) and $Nb_2(PO_4)_3$.

(ii) Topological analogs of the Na_2ZrSiO_5 framework are found in the synthetic phases $(TiO)SO_4$, $TaVO_5$ and MPO_5 (*M* = W, Nb, Ta).

(iii) The TIT framework $TiSiO_5$ is revealed in the structures of hydrosulfates of divalent metals H_2MSO_5 (*M* = Mg, Mn, Fe, Co, Ni, Zn).

(iv) Topological analogs of the *MT* layer $[ZrSi_2O_8]_{2\infty}$ in $Na_3HZrSi_2O_8$ occur in Zr systems {in molybdate $ZrMo_2O_8$ = $Zr(MoO_4)_2$ [CC = 65512], and the phosphate $Zr(HPO_4)_2(H_2O)$ [CC = 10258]} and in perchlorates $M(ClO_4)_2$ (*M* = Co, Ni) [CC = 33288, 33289].

In addition to performing a general classification, the methodology considered allows one to discover numerous variants of structural relationship (including the incomplete similarity within several coordination spheres) for small groups or separate pairs of compounds. The topological equivalence of crystallographically independent fragments of the same *MT* framework can also be detected. In this respect the structure of Na_2ZrSiO_5 is an interesting example of the topological decomposition of the *MT* framework on two equivalent *MT* layers (100). The *MT* layers (Fig. 8) united to the *MT* framework by O bridges [O2 and O4 atoms] are composed with topologically equivalent sets {Zr1, Si1, O1,5,7,9} and {Zr2, Si2, O3,6,8,10}.

A vivid demonstration of the advantages of the analytical CS method, when structure visualization is not required, is the topological analogy of alkaline silicates with the MT_2O_7 framework, but different space groups, unit-cell sizes and numbers of occupied Wyckoff orbits (the minerals pKEL and KHI, and the synthetic phase $Na_2SiSi_2O_7$). Note the topological similarity between zirconosilicates and three of four known high-pressure Si phases, and originality of $Na_2SiSi_3O_9$ topological type.

Of the PMEs with the minimum $N_3 = 15$, the first zirconosilicate with the UMB framework (Table 6) is unique by physicochemical properties. An important feature of its topology is the channels of ionic transportation, whose minimum section is formed by eight edges of *M* and *T* polyhedra (Ilyushin, 1993). The hydrothermal synthesis of this mineral was performed by Ilyushin & Demianets (1996, 1997). At present the ion-exchange properties of *A* subnets in $K_2ZrSi_3O_9(H_2O)_2$ with the UMB *MT* framework (substitution of K atoms with Na or Cs atoms) are being intensively studied (Poojary *et al.*, 1997; Jale *et al.*, 1999; Lin *et al.*, 1999) and have already resulted in the structurally investigated phases, whose chemical composition was modified by ion exchange up to $Na_2ZrSi_3O_9(H_2O)$ [CC = 84314], $NaCsZrSi_3O_9(H_2O)$ [CC = 84315] or $CsKZrSi_3O_9(H_2O)$ [CC = 84312]. In the two last zirconosilicates Cs atoms extrude Na and K atoms from small framework cavities, whereas Na atoms completely substitute K atoms forming the $Na_2ZrSi_3O_9(H_2O)$ phase. Note that this phase cannot be obtained by direct synthesis in the hydrothermal system Na–Zr–Si–O–H (Ilyushin *et al.*, 1983). Therefore, the three phases obtained by ion exchange in known frameworks are listed in the classification tables together with the method of their synthesis. Completely Zr-substituted silicates were obtained for *M* = Ti [$K_2TiSi_3O_9(H_2O)$, CC = 83587] and *M* = Sn [$K_2SnSi_3O_9(H_2O)$; Lin *et al.*, 1999]. All the compounds considered form the topological family of zeolitic UMB frameworks. In this set of topologically ideal frameworks the isomorphism Zr–Sn–Ti was found. In the case of frameworks with gaps the isomorphism Zr–Sn–Ti–Si was revealed for silicates of the LOV topological family.

6.5. Topological features of zirconosilicates with *R* = 7–11: *MT* frameworks with O gaps and *MT* layers

Note beforehand that referring the compounds with *R* = 7–11 (Table 8) to zirconosilicates is rather relative. These structures are formed from more than one chemical type of *M* atom. Therefore, in addition to the ordinary model of an *MT* framework consisting of ZrO_6 octahedra and SiO_4 tetrahedra,

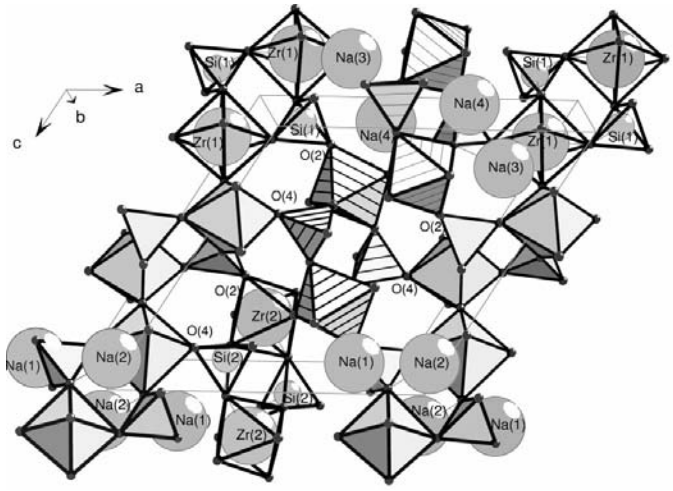

Figure 8
Topologically equivalent *MT* layers (100) in the *MT* framework of Na_2ZrSiO_5. A side view.

topologically more complex variants of its structure were considered which were constructed by sequentially adding the atoms with octahedral coordination, such as V, Ti, Y, Fe and Mn, to the list of framework-forming *M* atoms. Using these variants one can often select framework-forming *M* atoms in controversial cases. For this purpose it is necessary to find a topological relationship between one of the variants of framework composition and a framework, for which referring to atoms as framework-forming is unambiguous. The structural relationship between HIO and LAV (the variant II) was revealed in this way only when Zr atoms in LAV were considered as *M* atoms (Table 8). In our opinion, this circumstance allows one to exclude Fe atoms from the LAV framework and to calculate the *q* and *w* values for LAV given in Table 1.

For *MT* frameworks of this group 'special' PME types (designated as *sp-N*) are typical, where *M* polyhedra share their edges or have terminal O vertices (Fig. 9). For *M* ensembles containing terminal O vertices *A* and *B* atoms are also given to be in the local environment of O atoms. The number of such blocking atoms is found to be equal to three in all cases. In our opinion, the results obtained on the topological properties of PME structures for all chemical sorts of *M* atoms and modelling framework topological types allow the correction in a number of cases the description and structural–genetic relations accepted earlier for these substances. In particular, in structural mineralogy (Bokij, 1996) the phases ROS, LAV and HIO are referred to the woehlerite family; moreover, ROS falls also in the seidozerite family. Such correlations were established in view of similar unit-cell volumes (710–770 Å^3) and the stable Si_2O_7 group, typical for all these minerals. The data on CSs and visualization of PMEs for all *M* atoms allow the following statements to be made:

(i) ROS with three types of *M* nodes occupied by Zr, Ti and Mn atoms cannot fall in the SEI or WOE topological types, which comprise three and two types of *M* nodes, respectively, with other $\{N_k\}$.

(ii) WOE has no analogs among the above-mentioned phases. Its crystal structure is characterized by two types of *M* nodes completely occupied by Zr and V(+5) atoms. The topological properties of PMEs of V atoms with $N_{1-3} = \{6, 4, 13\}$ are of special interest. Such a PME type contains four *T* tetrahedra and two terminal O nodes.

(iii) In HIO the *M* positions are regularly occupied by Zr and Y atoms which possess non-trivial topological symmetry.

(iv) The LAV structure can be considered as a variant of the HIO structure. It can be derived from the HIO structure by substituting Y atoms with Zr atoms, *i.e.* HIO is a LAV superstructure. Thus, these two silicates form the topological family LAV–HIO (Nos. 38*a* and *b* in Table 1).

(v) SEI with three types of topologically different *M* nodes have no structural analogs among phases with $R = 7$ (Table 1). Another feature of its structure is the edge condensation of Zr octahedra with $N_{1-3} = \{6, 8, 25\}$, which was previously detected only in $Ca_3ZrSi_2O_9$ (the BAG family, $R = 4$, Table 1). Thus, such condensation is detected only in two of 41 topological types.

(vi) The mineral burpalite with $R = 7$ sometimes to be related to the families WOE or CUP (Bokij, 1996) is a phase with substitution of a part of Ca atoms with Na atoms in the basic structure $Ca_3ZrSi_2O_9$ (BAG family, Table 1). *MT*-condensed framework in BAG possesses by unique topology of Zr-nodes (Table 6) that reflects the presence of four polyhedra connected with the central *M*-octahedron in the PME.

The topological characteristics and PME composition for the phases considered above (Table 9) show that among all structures with different chemical sorts of *M* nodes Zr nodes have the strongest connectivity with Si tetrahedra. This important fact is an additional illustration of the leading crystal structural role of Zr-PMEs in the formation of *MT* frameworks. In this connection *MT* layer structures of the EVD family considered below ($R = 8$–11) with an abnormally high number of representatives for such large *R* are not exceptions. All these phases require a detailed chemical, geometrical and topological analysis of their crystal structures. The reasons are considered below why four compounds are referred to the same topological family 42(*a*)–(*d*) (Table 1) in

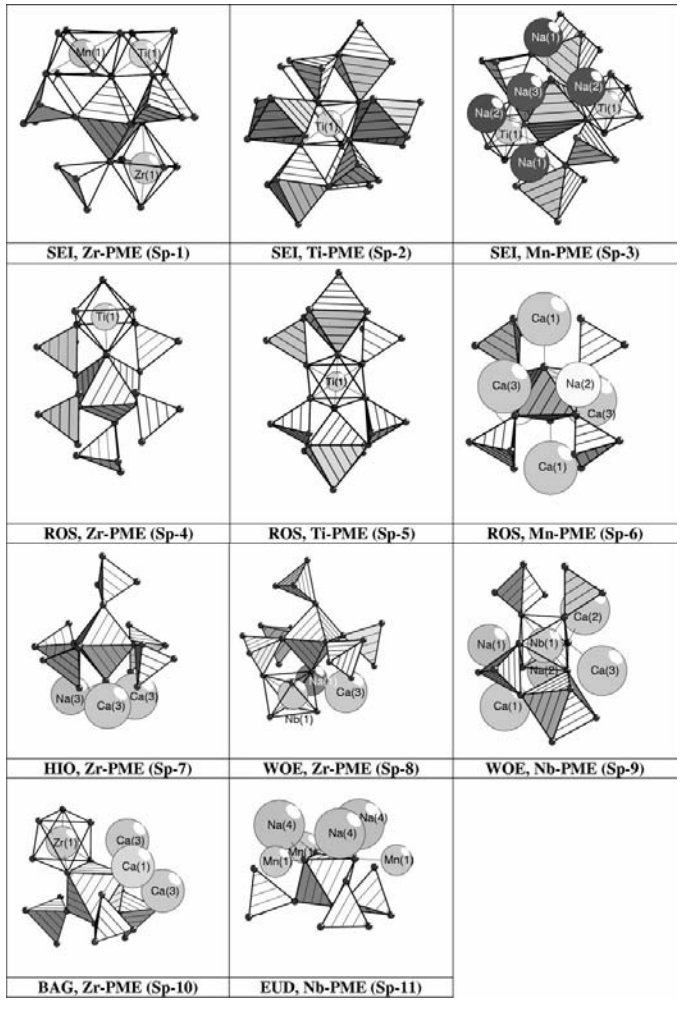

Figure 9
'Special' PME types (*sp-N*) typical for *MT* layers and *MT* frameworks with complex composition ($R = 7$–10), where *M* polyhedra share their edges or have terminal O vertices. *A* and *B* atoms blocking terminal O atoms of central *M* polyhedra are shown as well.

Table 9
Detailed composition of the second coordination sphere of *M* atoms in the *MT* frameworks given in Table 8.

In the composition of the coordination sphere all O atoms are terminal.

Topological type (family)	*M* atom	N_2	Composition of coordination sphere
SEI	Zr	8	5(Si) + 1(Zr) + 1(Ti) + 1(Mn)
	Ti	8	4(Si) + 2(Mn) + 2(Zr)
	Mn	6	2(Si) + 2(Ti) + 2(Zr)
ROS	Zr	6	5(Si) + 1(Ti)
	Ti	6	4(Si) + 2(Zr)
	Mn	4	4(Si) + 2(O)
WOE	Zr	6	5(Si) + 1(Nb)
	Nb	4	3(Si) + 1(Zr) + 1(O)
LAV–HIO	Zr(Y)	5	5(Si) + 1(O)
EUD–ONE–KEN	Zr	6	6(Si)
	Nb	6	3(Si) + 3(O)

spite of essential distinctions in the topological properties and chemical composition (R = 7–10) of their crystal structures.

The EVD structure type has no analogs among the other silicates considered here because of extremely high R values. However, in spite of such complex chemical composition the eudialite-like zirconosilicates are rock-forming with magmatic origin (Bokij, 1981, 1996), *i.e.* they are crystallized from melt. Recently Johnsen & Grice (1999) performed a systematic and complex research of 17 EVD phases of different composition. The precise determination of their crystal structures allowed them to decide a number of essential crystal structure problems for the phases of this family, such as clearing up the nature of the main chemical substitutions and calculation of the numbers of anions and cations of different types. Johnsen & Grice (1999) separated three new phases with superstructural atomic ordering in individual mineral species as the last members of the solid-state solution series (Table 1).

We have analyzed topological models for the basic eudialite crystal structure of $Na_{12}Ca_6Fe_3Zr_3Si_{24}O_{69}(OH)_3Cl_2$ (R = 8), which was independently solved in different space groups as non-centrosymmetric ($R3m$ model; Golyshev *et al.*, 1971) and centrosymmetric ($R\bar{3}m$ model; Giuseppetti *et al.*, 1971). New representatives of this family (Table 1) with essentially a more complex chemical composition [KEN (R = 9; Johnsen *et al.*, 1998; Johnsen & Grice, 1999) and ONE with new non-centrosymmetric $R3$ model (R = 10; Johnsen *et al.*, 1998)] have also been considered. Note that the centrosymmetric Ti analog of eudialite is known as the mineral alluaivite ($R\bar{3}m$ model with doubling along the c axis; Rastsvetaeva *et al.*, 1990; Bokij, 1996).

To analyze the topology of the EVD family phases we have applied the universal approach, where Zr octahedra and Si tetrahedra are assumed to be framework-forming units and all remaining atoms were considered as void-filling components, *i.e.* the atomic polyhedral model, typical for *A*,*B*-zirconosilicates, was used. Note that at the alternative description of the EVD crystal structure some authors (Johnsen & Grice, 1999; Bokij, 1996) selected Ca(Ca,Mn) rings of polyhedra connected with each other by isolated Fe(Mn) polyhedra in a layer to be a 2:1 package framed from each side with Si,O radicals. Then these Ca,Mn,Fe,Si,O packages are united in a three-dimensional framework by Zr octahedra.

A geometrical model explaining topological features of the structure of *all* EVD phases is an invariant *MT* layer $3[ZrSi_8O_{24}]_{2\infty} = [Zr_3Si_{24}O_{72}]_{2\infty}$ (three-layer package $4T$–M–$4T$), which contains all O atoms of the crystal structure (Fig. 10). The charge of the layer is compensated by Na^+, Ca^{2+}, Mn^{2+} and Fe^{2+} atoms possessing different superstructural ordering (Johnsen & Grice, 1999). Three terminal OH groups in nine T rings inside the layer are condensation centers for additional M and T polyhedra. They are complementary to an edge of the SiO_4 tetrahedron or edges of MO_6 octahedra (M = Nb in ONE and M = W, Nb in KHO with R = 11). The arrangement of additional T and M polyhedra in the basic layer can have different superstructural ordering.

To clear up the correspondence between the numbers of M, T and O atoms in the *MT* package let us consider the possible mechanisms of the modification of package PBUs resulting in an increase in the number of oxygen atoms up to 73, 74, 75, 76 or 78.

6.5.1. Modification of *MT* package with one PBU. The two limiting cases of the MT_8 layer modification by the only T or M polyhedron are as follows:

(i) T modification: $T + Zr_3Si_{24}O_{72} = Zr_3Si_{25}O_{73}$ (T = Si, increase of O atoms in the package rides the appearance of an additional terminal O atom after embedding the T tetrahedron into the package);

(ii) M modification: $M + Zr_3Si_{24}O_{72} = Zr_3MSi_{24}O_{75}$ (increase of O atoms in the package is maximum: three additional terminal O atoms appear).

6.5.2. Modification of *MT* package with two PBUs. In the case of simultaneous modification of the MT_8 layer by T and M polyhedra the layer composition can be found as a combination of successive M,T modifications:

(i) $2T$ modification: $2T + Zr_3Si_{24}O_{72} = Zr_3Si_{26}O_{74}$;

(ii) MT modification: $M + T + Zr_3Si_{24}O_{72} = Zr_3MSi_{25}O_{76}$;

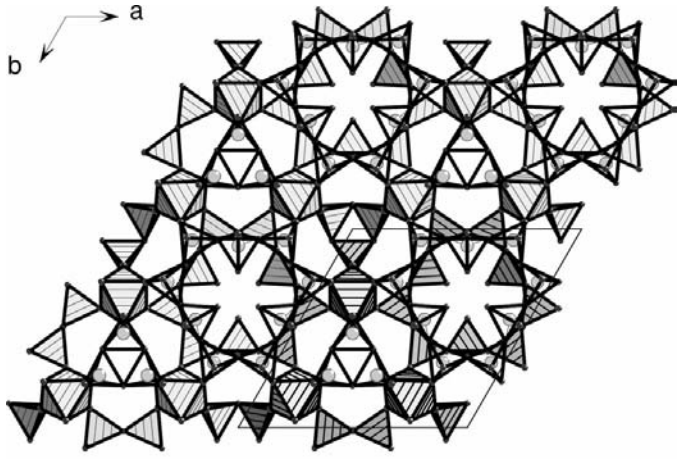

Figure 10
*XY*0 projection of the *MT* three-layer package $[Zr_3Si_{24}O_{72}]_{2\infty}$ in the EUD crystal structure.

(iii) $2M$ modification: $2M + Zr_3Si_{24}O_{72} = Zr_3M_2Si_{24}O_{78}$.

The composition $Zr_3MSi_{25}O_{76}$ (MT modification, M = Nb) is found in KEN as $Zr_3NbSi_{25}O_{74}(H_2O)_2$, where the water molecules should be considered as bonded with octahedral Nb atoms, not zeolitic. The maximum content of O atoms in the layer can be gained in hypothetical $Zr_3M_2Si_{24}O_{78}$ ($2M$ modification), when all nine T rings are modified with M octahedra.

The analysis of crystal structures of EVD and all other phases with R = 7–10 indicate that the complication of chemical composition (R > 6) makes impossible the construction of topologically ideal MT frameworks (without O gaps) because of the appearance of O vertices which are sterically inaccessible for mutual condensation. In this connection the most typical example is the EVD structure. OH groups inside the MT_8 package and all the terminal O vertices separated by layers of the A and B atoms superstructurally ordered in the ONE crystal structure are unavailable for the layer condensation. OH nodes play the role of chemically modifying centers in the EVD MT package, while the A,B superstructures consisting of Na, Ca, Sr, Mn and Fe atoms are formed with O nodes.

Topological modification of the MT_8 package and the appearance of additional M, T and O vertices result in varying N_k values and, strictly speaking, in another topology of the modified package. However, the topological properties of the package base (when modifying M and T polyhedra are forgotten) remain the same. Therefore, we consider all compounds of the EVD family as topologically close structure types.

The only example of a layer MT structure among the phases with simpler chemical composition (R = 3–6, Table 6) is $Na_3HZrSi_2O_8$, whose natural analog is $Ca_3MgSi_2O_8$ (MRW). In this compound the terminal O atoms of the T tetrahedra lie above and below the plane of the MT_2O_8 package. Ca atoms in MRW as well as in EVD fill the space between MT_2O_8 layers. Na atoms play a similar role in the crystal structure of $Na_3HZrSi_2O_8$. Note that the MT_2 layer with the MRW topology requires no necessary presence of modifying A or B atoms for its creation at the initial stages of PME precursor formation, because it is reproduced in different Zr compounds, for instance in the aforementioned $ZrMo_2O_8$ and $Zr(HPO_4)_2(H_2O)$. In the case of the EVD crystal structure the PME precursors are formed with the participation of Na atoms located inside the package between Zr octahedra and, according to our results, are kept permanently in all chemically and topologically modified phases studied by Johnsen & Grice (1999).

7. Conclusion

Thus, the study of MT frameworks shows their essential topological variety. There were 93 zirconosilicates investigated and their MT analogs were arranged in 21 topological families and 20 topological types with unique topologies of M nodes; 54 topological types of T node were found. There were 35 of 41 topological types and families including 33 MT frameworks and two MT layers which comprise zirconosilicates. Six remaining topological types (not families) are represented by one Na,Si[6] silicate, one Ca,Sn silicate and four A(B),Ti silicates. As a rule, for the identification of an MT framework it is sufficient to determine the topological properties of one topological type of M-node within the first ten coordination spheres.

Analysis of the frequencies for the types of M nodes keeps two important problems unsolved. The first one is why only half (six of 12) of the possible types of MT_6 ensembles is revealed among 30 topological types of MT frameworks, while the connectivity of T–T contacts does not exceed six (at the same time the theoretically constructed MT_6 ensembles can be characterized by the higher values P_6 = 8, 10, 12). The second one is that in about half (13 of 30) of the topologically ideal MT frameworks, only one type of ensemble with the value P_6 = 0 is realised, and the distribution of the remaining types (five types of 12 possible ones) depending on their frequencies is extremely non-uniform. These interrelated problems should be solved by creating the structure formation model for the topological types of natural zirconosilicates. This model should be based on the treatment of space correlations between framework-forming MT nodes (*i.e.* of their long-range order) and on the definition of selection rules controlling the processes of PME formation by symmetry and topology. It should include the universal model of formation and evolution of MO_6 and TO_4 PBU polyhedra in non-equilibrium systems, whose behavior is determined by large-scale fluctuations of particle density. The accent in such systems should be moved from the concrete *geometrical forms* of the particles composing crystal structure (which can be both identical and various) to the *elementary events* in which these particles are involved. Namely, the sequences of elementary events should be modelled which result in nucleation of initial MT nodes and in their evolution to three-dimensional periodic structure. Thus, the fundamental parameters of the models should be the most general properties of the PBU systems, such as space symmetry (crystallographic or non-crystallographic) and the PME topological properties characterized by CSs of M, T and, if necessary, O nodes.

APPENDIX *A*
Some basic concepts

Coordination sequence (CS) of an A atom in a net containing atoms A, B, C *etc.* is a set of integers $\{N_k\}$, where N_k is the number of adjacent atoms in the kth coordination sphere of A, *i.e.* of all the atoms A, B, C *etc.* connected directly with the atoms of the $(k-1)$th sphere, except the atoms of internal $(k-2)$th sphere. The original atom A itself composes formally the zero coordination sphere.

Reduced graph (RG) is a finite non-oriented graph derived from the graph of a three-dimensional net of crystal structure by closing edges, extending outside the unit-cell boundaries on the translationally equivalent atoms being inside the unit cell or on its boundary. In general, RG is a labeled multigraph with loops. The labels at loops and multiple edges indicate with

what translationally equivalent vertices a given edge has been connected before the closing procedure. The number of RG vertices is exactly equal to the number of atoms in the unit cell. RG corresponds to the initial infinite graph of a three-dimensional net accurate to isomorphism.

Connected substructure (CSS) is a subset of net nodes keeping connectivity between them. All the net nodes not belonging to this subset are to be contracted to the subset nodes (Fig. 1*a*). The CSS subnet comprises only direct bonds between nodes of the subset, which form a subset of bonds in the original net (all net nodes not belonging to the subnet are to be removed together with their bonds, see Fig. 1*b*).

Topological representation (TR) of crystal structure is a set of connected substructures constructed for complexing atoms under the stipulation that remaining atoms are either contracted to complexing atoms or removed together with their bonds.

Topological type is a set of compounds with the same topology of reduced graphs for their crystal structures. A topological type is given a name of one of its representatives, from which the ancestor of one of the known structure types can be selected. Following the mineralogical traditions we herein use the term ***topological family*** for designating a topological type, which composes more than one representative.

Primary building unit (PBU) is an elementary polyhedral component of an *MT* framework: MO_6 octahedron or TO_4 tetrahedron.

MT framework is a three-dimensional net formed by condensation of *M* octahedra [MO_6] and *T* tetrahedra [TO_4]. In a ***topologically ideal MT framework*** all O atoms are bridged and PBUs have only common vertices. Another type of *MT* framework is an ***MT framework with O gaps*** which contains terminal O atoms. In *MT* frameworks of this type PBUs can connect together by both vertices and edges. As crystal structures with edge condensation of *M* octahedra are accumulated, an additional set of ***MT-condensed frameworks*** would be separated.

Polyhedral microensemble (PME) is a cluster consisting of several PBUs; its form reflects spheroidal layer-by-layer growth of an *MT* framework starting from a central node-nucleator. The PME of the first sublevel (PME-1) is formed from the central TO_4 tetrahedron or MO_6 octahedron and, respectively, from four or six TO_4 and/or MO_6 polyhedra connected with the central polyhedron by O vertices. PME of an *i*th sublevel (PME-*i*) is to be derived from PME of the $(i-1)$th sublevel by condensation of an additional spheroidal PBU layer through terminal O vertices. Each new PME sublevel corresponds to two coordination spheres of central *M* or *T* nodes, one of which comprises only O nodes and another consists of only *M*,*T* nodes.

Suprapolyhedral invariant (SPI) is a cluster consisting of several geometrically different PBUs (octahedra and/or tetrahedra), typical for the group of topologically non-equivalent *MT* frameworks. PMEs and SBUs (in zeolites) are special cases of SPIs.

References

Aslanov, L. A. (1988). *Acta Cryst.* B**44**, 449–458.
Bader, R. F. W. (1990). *Atoms in Molecules – a Quantum Theory*. Oxford University Press.
Barrer, R. M. (1982). *Hydrothermal Chemistry of Zeolites*. New York: Academic Press.
Belov, N. V. (1959). *Crystal Chemistry of Large Cation Silicates*. New York: Consultant Bureau.
Belov, N. V. (1976). *Essays on Structural Mineralogy*. (In Russian). Mocsow: Nedra.
Blatov, V. A. (2000). *Acta Cryst.* A**56**, 178–188.
Blatov, V. A. (2001). *Z. Kristallogr.* **216**, 165–171.
Blatov, V. A. & Serezhkin, V. N. (2000). *Russ. J. Inorg. Chem.* Suppl. S105–S220.
Blatov, V. A., Shevchenko, A. P. & Serezhkin, V. N. (2000). *J. Appl. Cryst.* **33**, 1193.
Bokij, G. B. (1981). Editor. *Minerals: Handbook.*, Vol. III, pt 2. Moscow: Nauka.
Bokij, G. B. (1992). Editor. *Minerals: Handbook*, Vol. IV, pt 1 and 2. Moscow: Nauka.
Bokij, G. B. (1996). Editor. *Minerals: Handbook*, Vol. IV, pt 3. Moscow: Nauka.
Bokij, G. B. (1998). *Systematics of Natural Silicates*. Moscow: VINITI.
Bragg, W. L. (1930). *Z. Kristallogr.* **74**, 237–305.
Breck, D. W. (1974). *Zeolite Molecular Sieves. Structure, Chemistry and Use*. New York: Wiley-Interscience.
Brunner, G. O. & Laves, F. (1971). *Wiss. Z.. Techn. Univ. Dresden*, **20**, 387–390.
Cheetham, A. K., Ferey, G. & Loiseau, T. (1999). *Angew. Chem. Int. Ed.* **38**, 3268–3292.
Christofides, N. (1975). *Graph Theory. An Algorithmic Approach*. New York: Academic Press.
Clearfield, A. (2001). *Solid State Sci.* **3**, 103–112.
Ferreira, P., Ferreira, A., Rocha, J. & Sousa, M. R. (2001). *Chem. Mater.* **13**, 355–363.
Giuseppetti, G., Mazzi, F. & Tadini, C. (1971). *Tschermaks Miner. Petrogr. Mitt.* **16**, 105–127.
Golyshev, V. M., Simonov, V. I. & Belov, N. V. (1971). *Kristallographiya*, **16**, 93–98.
Grosse-Kunstleve, R. W., Brunner, G. O. & Sloane, N. J. A. (1996). *Acta Cryst.* A**52**, 879–889.
Hawthorne, F. C. (1983). *Acta Cryst.* A**39**, 724–736.
Hawthorne, F. C. (1985). *Am. Mineral.* **70**, 455–473.
Hawthorne, F. C. (1990). *Z. Kristallogr.* **192**, 1–52.
Hawthorne, F. C. (1994). *Acta Cryst.* B**50**, 481–510.
Hong, H. Y.-P. (1976). *Mater. Res. Bull.* **11**, 173–182.
Ilyushin, G. D. (1989). *Sov. Phys. Crystallogr.* **34**, 506–510.
Ilyushin, G. D. (1993). *Neorgan. Mater.* **29**, 971–975.
Ilyushin, G. D. & Demianets, L. N. (1989). *Germanates of Four-Valent Metals*. (In Russian.) Moscow: VINITI.
Ilyushin, G. D. & Demianets, L. N. (1996). *Growth of Crystals*, edited by E. I. Givargisov and A. M. Melnikova, Vol. 20, pp. 89–102. New York: Consultant Bureau.
Ilyushin, G. D. & Demianets, L. N. (1997). *Crystallogr. Rep.* **42**, 1124–1129.
Ilyushin, G. D. & Demianets, L. N. (2001). *Crystallogr. Rep.* **46**, 801–809.
Ilyushin, G. D., Demianets, L. N., Ilyukhin, V. V. & Belov, N. V. (1983). *Dokl. Akad. Nauk.* **28**, 603–605.
Ilyushin, G. D., Khomyakov, A. P., Shymyatskaya, N. G., Voronkov, A. A., Nevskii, N. N., Ilyukhin, V. V. & Belov, N. V. (1981*a*). *Dokl. Akad. Nauk.* **26**, 118–119.
Ilyushin, G. D., Pudovkina, Z. V., Voronkov, A. A., Khomyakov, A. P., Ilyukhin, V. V. & Pyatenko, Yu. A. (1981*b*). *Dokl. Akad. Nauk.* **26**, 257–258.
Ilyushin, G. D., Voronkov, A. A., Ilyukhin, V. V., Nevskii, N. N. & Belov, N. V. (1981*c*). *Dokl. Akad. Nauk.* **26**, 808–810.

Ilyushin, G. D., Voronkov, A. A., Nevskii, N. N., Ilyukhin, V. V. & Belov, N. V. (1981*d*). *Dokl. Akad. Nauk.* **26**, 916–917.
Jale, S. R., Ojo, A. & Fitch, F. R. (1999). *Chem. Commun.* pp. 411–412.
Johnsen, O., Gault, R. A., Grice, J. D. & Ercit, T. S. (1999). *Can. Miner.* **37**, 893–899.
Johnsen, O. & Grice, J. D. (1999). *Can. Miner.* **37**, 865–891.
Johnsen, O., Grice, J. D. & Gault, R. A. (1998). *Eur. J. Miner.* **10**, 207–219.
Johnsen, O., Grice, J. D. & Gault, R. A. (1999). *Can. Miner.* **37**, 1295–1301.
Khomyakov, A. P. (1995). *Mineralogy of Hyperagpaitic Alkaline Rocks.* Oxford University Press.
Kostov, I. (1971). *Sov. Phys. Crystallogr.* **16**, 1220–1224.
Liebau, F. (1956). *Phys. Chem.* **206**, 73–92.
Liebau, F. (1985). *Structural Chemistry of Silicates: Structure, Bonding and Classification.* Springer: Berlin.
Lin, Z., Rocha, J. & Valente, A. (1999). *Chem. Commun.* **24**, 2489–2490.
Masse, R. & Durif, F. (1973). *C. R. Acad. Sci. Paris Ser. C*, **276**, 1029–1032.
Meier, W. M. (1968). *Molecular Sieves*, pp. 10–27. London: Society of Chemistry and Industry,
Meier, W. M. & Moeck, H. J. (1979). *J. Solid State Chem.* **27**, 349–355.
Meier, W. M., Olson, D. H. & Baerlocher, C. (1996). Editors. *Atlas of Zeolite Structure Types*, 4th ed. Amsterdam: Elsevier.
Nosirev, N. A., Treushnikov, E. N., Ilyukhin, V. V. & Belov, N. V. (1974). *Dokl. Akad. Nauk.* **218**, 830–832.
O'Keeffe, M. (1995). *Acta Cryst.* A**51**, 916–920.
Poojary, D. M., Bortun, A. I., Bortun, L. N. & Clearfield, A. (1997). *Inorg. Chem.* **36**, 3072–3079.
Puschcharovskii, Yu. D. (1986). *Structural Mineralogy of Silicates and Their Synthetic Analogs.* (In Russian.) Moscow: Nedra.
Rastsvetaeva, R. K., Khomyakov, A. P., Andrianov, V. I. & Gusev, A. I. (1990). *Dokl. Akad. Nauk.* **312**, 1379–1383.
Rocha, J. & Anderson, M. W. (2000). *Eur. J. Inorg. Chem.* **5**, 801–818.
Quintana, P. & West, A. R. (1981). *Mineral. Mag.* **44**, 361–362.
Smith, J. V. (1988). *Chem. Rev.* **88**, 149–182.
Stixrude, L. & Bukowinski, M. S. T. (1990). *Am. Mineral.* **75**, 1159–1169.
Zoltai, T. (1960). *Am. Mineral.* **45**, 960–973.